

(2)

# NAVAL POSTGRADUATE SCHOOL

## Monterey, California

AD-A231 491

DTIC FILE COPY



DTIC  
SELECTED  
FEB 04 1991  
S B D

# THESIS

MEASUREMENTS ON LASER PRODUCED  
PLASMA USING FARADAY-CUPS

by

Youn , Duck-Sang

December 1989

Thesis Advisor

Fred R. Schwirzke

Approved for public release; distribution is unlimited.

91 2 01 061

Unclassified

security classification of this page

REPORT DOCUMENTATION PAGE

1a Report Security Classification Unclassified		1b Restrictive Markings		
2a Security Classification Authority		3 Distribution, Availability of Report Approved for public release; distribution is unlimited.		
2b Declassification Downgrading Schedule				
4 Performing Organization Report Number(s)		5 Monitoring Organization Report Number(s)		
6a Name of Performing Organization Naval Postgraduate School	6b Office Symbol (if applicable) 61	7a Name of Monitoring Organization Naval Postgraduate School		
6c Address (city, state, and ZIP code) Monterey, CA 93943-5000		7b Address (city, state, and ZIP code) Monterey, CA 93943-5000		
8a Name of Funding Sponsoring Organization	8b Office Symbol (if applicable)	9 Procurement Instrument Identification Number		
8c Address (city, state, and ZIP code)		10 Source of Funding Numbers Program Element No Project No Task No Work Unit Accession No		
11 Title (Include security classification) MEASUREMENTS ON LASER PRODUCED PLASMA USING FARADAY-CUPS				
12 Personal Author(s) Youn . Duck-Sang				
13a Type of Report Master's Thesis	13b Time Covered From To	14 Date of Report (year, month, day) December 1989	15 Page Count 93	
16 Supplementary Notation The views expressed in this thesis are those of the author and do not reflect the official policy or position of the Department of Defense or the U.S. Government.				
17 Cosen Codes	18 Subject Terms (continue on reverse if necessary and identify by block number) Laser produced plasma, Velocities, Temperature, Faraday Cup measurements			
Field	Group	Subgroup		
19 Abstract (continue on reverse if necessary and identify by block number)				

Experiments were performed on laser produced plasma from Lexan targets in a vacuum chamber at pressures of a few times  $10^{-5}$  Torr. Plasma diagnostics was performed using Faraday-cups-biased at -50 volts to +105 volts DC. In analyzing 460 oscilloscope trace pictures of Faraday-cup signals, the plasma expansion velocities measured was determined to be  $1.25 \times 10^7 \text{ cm/sec}$ .

At a distance of 10 cm from the laser-target impact point, the plasma electron temperature was determined from Faraday cup measurement to be about 2.4 ev. The plasma density was approximately  $10^{13} \text{ cm}^{-3}$ .

20 Distribution Availability of Abstract <input checked="" type="checkbox"/> unclassified unlimited <input type="checkbox"/> same as report <input type="checkbox"/> DTIC users	21 Abstract Security Classification Unclassified	
22a Name of Responsible Individual Fred R . Schwirzke	22b Telephone (Include Area code) (408) 646-2635	22c Office Symbol 61Sw

DD FORM 1473.84 MAR

83 APR edition may be used until exhausted  
All other editions are obsolete

security classification of this page

Unclassified

Approved for public release; distribution is unlimited.

Measurements on Laser Produced Plasma Using Faraday-Cups

by

Youn , Duck-Sang  
Lieutenant Commander , Republic of Korea Navy  
B.S., Korean Naval Academy , 1979

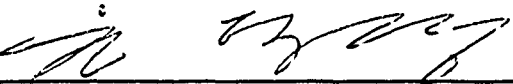
Submitted in partial fulfillment of the  
requirements for the degree of

MASTER OF SCIENCE IN PHYSICS

from the

NAVAL POSTGRADUATE SCHOOL  
December 1989

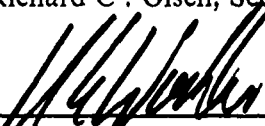
Author:

  
Youn , Duck-Sang

Approved by:

  
Fred R . Schwirzke, Thesis Advisor

  
Richard C . Olsen, Second Reader

  
Karlheinz E . Woehler, Chairman,  
Department of Physics

## ABSTRACT

Experiments were performed on laser produced plasma from Lexan targets in a vacuum chamber at pressures of a few times  $10^{-5}$  Torr. Plasma diagnostics was performed using Faraday-cups biased at -50 volts to +105 volts DC. In analyzing 460 oscilloscope trace pictures of Faraday-cup signals, the plasma expansion velocities measured was determined to be  $1.25 \times 10^7 \text{ cm/sec}$ .

At a distance of 10 cm from the laser-target impact point, the plasma electron temperature was determined from Faraday cup measurement to be about 2.4 ev. The plasma density was approximately  $10^{13} \text{ cm}^{-3}$ .



Accession For	
NTIS GRA&I	<input checked="" type="checkbox"/>
DTIC TAB	<input type="checkbox"/>
Unannounced	<input type="checkbox"/>
Justification	
By _____	
Distribution/	
Availability Codes	
Dist	Avail and/or Special
A-1	

## TABLE OF CONTENTS

I. INTRODUCTION .....	1
II. BACKGROUND AND THEORY .....	3
A. INTRODUCTION .....	3
B. LASER - TARGET INTERACTIONS .....	3
C. PLASMA - SURFACE INTERACTIONS .....	4
1. Debye Shielding Length .....	4
2. Sheaths Effect .....	6
3. Child - Langmuir Law .....	9
D. ELECTROSTATIC PROBE AND FARADAY - CUP MEASUREMENTS .....	10
III. EXPERIMENTAL EQUIPMENT AND PROCEDURES .....	14
A. INTRODUCTION .....	14
B. EXPERIMENTAL APPARATUS .....	14
1. Laser .....	14
2. Vacuum System .....	14
3. Optics .....	16
4. Energy Meter .....	17
5. Oscilloscope .....	17
6. Detector Assembly .....	17
7. Experimental Set - Up .....	19
C. EXPERIMENTAL PROCEDURE .....	25
1. Target Description and Preparation .....	25
2. Energy Measurements .....	25
3. Faraday Cup Signal Measurements .....	25
IV. EXPERIMENTAL RESULTS .....	27

A. MEASUREMENT ON LASER PRODUCED PLASMA .....	27
1. Ionization and Sparking in An Electric Field .....	27
2. Response Signal as Function of Distances .....	30
3. Measurements Parallel and Perpendicular to Streaming Plasma	32
4. Difference of Signals between Various Detectors .....	40
B. EVALUATION OF PLASMA PARAMETERS .....	42
1. Plasma Expansion Velocity .....	42
2. Measurement of Electron Temperature .....	44
3. Plasma Density .....	49
 V. SUMMARY AND DISCUSSION OF RESULTS .....	57
A. SUMMARY OF RESULTS .....	57
B. DISCUSSION OF RESULTS .....	57
 VI. CONCLUSION AND RECOMMENDATIONS .....	60
 APPENDIX A. LUMONICS TE-822 HP CO <sub>2</sub> LASER OPERATING PROCEDURE .....	61
1. Laser Enclosure Cover Interlocks (2) .....	61
2. Laser Output Port Protective Cover Interlock .....	61
3. Cooling Water Flow .....	62
4. Laser Power Key .....	62
5. Gas on / off Switch .....	62
6. Plasma Laboratory Door .....	62
A. LASER SYSTEM START-UP .....	62
B. LASER SYSTEM SHUT DOWN PROCEDURES: .....	67
 APPENDIX B. VEECO 400 VACUUM SYSTEM OPERATING PROCEDURES .....	68
A. VACUUM SYSTEM START-UP .....	68
B. HIGH VACUUM CHAMBER OPERATION .....	70

C. OPENING THE CHAMBER .....	70
D. SYSTEM IDLING CONDITION .....	71
E. SHUT DOWN THE SYSTEM COMPLETELY .....	71
APPENDIX C. SINGLE LANGMUIR PROBES .....	73
LIST OF REFERENCES .....	77
INITIAL DISTRIBUTION LIST .....	79

## LIST OF TABLES

Table 1. VOLTAGE , CURRENT , CURRENT DENSITY MEAS- URED WITH FARADAY CUP WITH ONE ENTRANCE HOLE ( D=10CM ) .....	55
Table 2. VOLTAGE, CURRENT, CURRENT DENSITY MEASURED WITH FARADAY CUP WITH 4 SMALL ENTRANCE HOLES (D=10CM ) .....	56

## LIST OF FIGURES

Figure 1. Plasma - Wall Interaction .....	8
Figure 2. Lumonics TE-822 HP CO <sub>2</sub> Laser .....	15
Figure 3. VEECO 400 Vacuum System .....	16
Figure 4. RJ-7000 Energy Meter and RJP-700 Probe .....	18
Figure 5. Faraday Cup Schematic .....	21
Figure 6. Circuit Schematic .....	21
Figure 7. Faraday Cup Cover Hole, Schematic .....	22
Figure 8. Comparison of Current Signals of Two Faraday Cups FC1 with 0.3 mm Entrance Hole and FC3 with 0.5 mm Hole. Bias V=-25 Volt .....	22
Figure 9. Two Kinds of Detector Rim, Schematic .....	23
Figure 10. Different Methods of Connection of Detector to BNC Cable ..	23
Figure 11. Configuration of Equipment .....	24
Figure 12. Sparking Potential (V) as a Function of The Reduced Electrode Distance Pd in Several Gases [Ref.14] .....	28
Figure 13. Distance 10 cm, Potential -20 V in Thin and Round Edge Faraday Cup .....	29
Figure 14. Distance 10 cm, Potential -20 V in Thick and Sharp Edge Faraday Cup .....	29
Figure 15. Peak Voltage vs Bias Voltage at Variable Distance ( Normal Faraday Cup) .....	31
Figure 16. Parallel Orientation of Faraday Cup .....	32
Figure 17. Peak Voltage vs Time at $\pm 5V$ Probe Voltage in Parallel Ori- entation (1-Electron Current, 2-Ion Current) .....	33
Figure 18. Peak Voltage vs Time at $\pm 10V$ Probe Voltage in Parallel Ori- entation (1-Electron Current, 2-Ion Current) .....	33
Figure 19. Peak Voltage vs Time at $\pm 20V$ Probe Voltage in Parallel Ori- entation (1-Electron Current, 2-Ion Current) .....	34

Figure 20. Peak Voltage vs Time at 30V Probe Voltage in Parallel Orientation (1-Electron Current, 2-Ion Current) .....	34
Figure 21. Peak Voltage vs Time at 40V Probe Voltage in Parallel Orientation (1-Electron Current, 2-Ion Current) .....	35
Figure 22. Perpendicular Orientation of Faraday Cup .....	36
Figure 23. Peak Voltage vs Time at 5V Probe Voltage in Perpendicular Orientation (1-Electron Current, 2-Ion Current) .....	37
Figure 24. Peak Voltage vs Time at 10V Probe Voltage in Perpendicular Orientation (1-Electron Current, 2-Ion Current) .....	38
Figure 25. Peak Voltage vs Time at 20V Probe Voltage in Perpendicular Orientation (1-Electron Current, 2-Ion Current) .....	38
Figure 26. Peak Voltage vs Time at 30V Probe Voltage in Perpendicular Orientation (1-Electron Current, 2-Ion Current) .....	39
Figure 27. Peak Voltage vs Time at 40V Probe Voltage in Perpendicular Orientation (1-Electron Current, 2-Ion Current) .....	39
Figure 28. Peak Voltage vs Bias Voltage at Variable Distance (Soldered Faraday Cup) .....	41
Figure 29. Distance Gap 5 cm, Probe Bias Voltage -20 V, in Parallel Orientation (Faraday Cup1-10cm from Target, FC2-5cm from Target) .....	45
Figure 30. Distance Gap 10 cm, Probe Bias Voltage -20 V, in Parallel Orientation (FC1-15cm, FC2-5cm) .....	45
Figure 31. Distance Gap 5 cm, Probe Bias Voltage +20 V, in Parallel Orientation (FC1-10cm, FC2-5cm) .....	46
Figure 32. Distance Gap 10 cm, Probe Bias Voltage +20 V, in Parallel Orientation (FC1-15cm, FC2-5cm) .....	46
Figure 33. Distance Gap 5 cm, Probe Bias Voltage +20 V, in Perpendicular Orientation (FC1-10cm, FC2-5cm) .....	47
Figure 34. Distance Gap 10 cm, Probe Bias Voltage +20 V, in Perpendicular Orientation (FC1-15cm, FC2-5cm) .....	47
Figure 35. Ln I <sub>e</sub> vs Probe Bias Voltage .....	48

Figure 36. Peak Voltage vs Bias Voltage (-20 V to +10 V ), Distance $d = 10\text{cm}$ .....	51
Figure 37. Current vs Bias Voltage (-10 V to +7 V ), Distance $d = 10\text{cm}$ ..	52
Figure 38. Peak Voltage vs Bias Voltage (0 v to +105 V ), Distance $d = 10\text{cm}$	53
Figure 39. Current vs Bias Voltage (0 V to +105 V ), Distance $d = 10\text{cm}$ .	54
Figure 40. VEECO Vacuum Chamber Controls .....	72
Figure 41. V-I Characteristics of Single Langmuir Probe .....	74

## ACKNOWLEDGEMENTS

I would like to express my gratitude and appreciation to professor Fred R. Schwirzke and Richard C. Olsen for their friendly advice and guidance in all phases of this research.

I wish to thank Mr. Robert Sanders for his assistance in the operation of the equipment in the Plasma Physics Laboratory, and the craftsman Mr. George Jaksha who supported this research throughout.

To my friends and colleagues Lieutenant Michael V. Hensen, and Richard K. Down, I offer my thanks for their reliable assistance and friendship during the experiment and this research.

Finally, I am grateful to my wife, Youn-Young, for her understanding and support throughout this work and my completion of studies at the NPS.

And thanks to my son, Hyun-sung for love and being healthy and patient for two and half years in Monterey, California.

## I. INTRODUCTION

Laser plasma production has been of interest to researchers since the early 1970's. The use of the laser as a scientific instrument quickly drew the attention of the academic community. Laser-target interaction soon became a topic of considerable research effort. Industrial and military applications of laser-dominated technology are considerable. The effort of high power laser interaction with matter include (1) heating [ Ref. 1] (2) melting, (3) vaporization of solid materials, (4) emission of charged particles, (5) emission of neutral particles (6) plasma production, (7) electrical discharge in gases produced by high energy laser interaction, and (8) application of these effects to material processing [ Ref. 2].

It is now understood that when solid targets are struck by a laser beam, some of the light energy is absorbed and a part is reflected, the amount of reflection being dependent on the target material and surface conditions [ Ref. 1].

The amount of radiant energy and the time-length of the laser pulse striking the target are the controlling parameters which determine the results of the interaction. If a plasma is formed, the absorbed energy is transferred through collisions to electrons and ions, and part of it heat the material.

Initially, the absorbed photon energy is, for all practical considerations, instantly turned to heat through particle collisions, rapidly heating a small quantity of surface material to very high temperatures. A laser pulse of sufficient energy will rapidly produce a plasma, a dense cloud of ionized particles.

Different types of Langmuir probes are widely used as diagnostic tools to investigate plasmas. Probe theories, depending upon the nature and parameters of the plasma, relate the measured value of the probe current ( or voltage ) to the plasma density, electron temperature, floating and plasma potentials and oscillations [ Ref. 3]. The shape and size of the selected probe depend upon the

plasma parameters and the quantity to be determined. Previous research at the Naval Postgraduate School (NPS) on laser produced plasma, particle velocity, and density was conducted using various diagnostic techniques.

Brooks used floating double probes, magnetic probes and quartz pressure probe. Peak plasma density measured in the main plasma was  $2.5 \times 10^{14} (cm^{-3})$  at the distance of 2.4 cm and the expansion velocity was  $1.1 \times 10^7$  cm/sec [Ref.4].

Callahan measured the plasma ion velocity of aluminum ions with a floating double electrostatic probe. The results were plasma velocities of  $5.6 \times 10^6$  cm/sec and plasma ion density varied from  $10^{11} (cm^{-3})$  to  $10^{13} (cm^{-3})$  for the streaming plasma [Ref. 5].

The Faraday cup is a metallic electrode (usually of cylindrical shape ), which is inserted into the plasma. From the current collected by the Faraday cup as a function of probe bias voltage, information can be obtained about the plasma density and temperature. Interpretation of the Faraday cup signals is usually complicated, however, because the current-voltage characteristic curve depends on the details of the plasma Faraday cup interaction, for example, the emission of secondary electrons.

A dense plasma is produced by focusing the pulsed  $CO_2$  laser light on the surface of a target suspended inside a vacuum chamber. The plasma expands and the thermal energy of the plasma is rapidly converted into directed ion motion. Finally, the plasma terminates at the wall of the vacuum chamber. The lifetime of such a plasma is quite short.

The objective of this experiment is to measure laser produced plasma parameters using Faraday cups.

## II. BACKGROUND AND THEORY

### A. INTRODUCTION

The irradiation of solid targets by high power lasers has been the subject of numerous research papers and reports which describe the thermal, mechanical, and electrical effects of laser target interactions. When a high power laser pulse is focused onto a solid surface, a high density plasma is formed. Much of the experimental and theoretical work done on this phenomenon has been directed to understanding the laser heating and plasma dynamics in the time during and shortly after the laser pulse, when the plasma is expected to be collisionally dominated and when the initially high temperature of the ions and electrons is being converted to the ordered kinetic energy of expansion.

A basic understanding of each of these processes and their interrelationships and relative importance is a necessary prerequisite before conducting experimental research.

### B. LASER - TARGET INTERACTIONS

Laser radiation absorption by a solid metal target causes heat to be deposited in a surface layer of the target material. The surface temperature increases and heat waves are propagated into the target. The heat cannot diffuse out of the absorbing target layer as fast as it is being injected so the temperature continues to increase until the target material begins to vaporize.

At the time of vaporization, the surface temperature of the target material will begin to depend on the rate of vaporization; that is, the evaporation mechanism. The thermal conductivity, heat capacity, and density are all temperature dependent. The reflectivity is temperature and thermodynamic phase dependent. At sufficiently high laser power density the blow off will be in the plasma state.

In addition to the thermal change to the target, there is a strong pressure built up on the target due to recoil from the vapor blow off.

The transition of a gas into the plasma state involves various particle interaction processes, collisions of the particles among themselves and interactions with radiation encompass most of the energy transfer [ Ref. 6]. Ionization, the stripping of electrons from atoms and molecules, is accomplished by the energetic ( hot ) electrons colliding with atoms and molecules. The inverse of this process is called recombination. The atom or molecule has to rid itself of energy. Three body recombination, in which two electrons collide simultaneously with an ion, one carrying away the excess energy and the other attaching itself, takes place in a dense plasma.

There are three basic methods of radiation emission from particle interactions in a plasma; discrete radiation, recombination radiation, and bremsstrahlung. Discrete radiation arises from electron transitions from one energy level to another in the same atom. Discrete radiation is of a single wave length. A complete picture of this form of radiation consists of numerous spectral lines.

Recombination radiation is emitted when a free electron is captured by an ion. A lower energy state is assumed by the electron and the energy is emitted in the form of a photon. Bremsstrahlung is radiation from interaction between a free electron and an ion in which the electron is only decelerated, not captured. This is referred to as free-free radiation.

## C. PLASMA - SURFACE INTERACTIONS

### 1. Debye Shielding Length

When a plasma is subjected to an external electric field the electrons and ions will drift in opposite directions. As they drift apart, they produce a charge separation and an internal electric field, which opposes the external field. The width of the region, over which the charge separation can occur to balance the

external electric field, is proportional to the thermal energy of the plasma particles. If the dimension of the bulk plasma is greater than the dimension of the region over which this charge separation occurs, the interior of the plasma will be shielded from the external field.

The width of the charge separation can be determined, approximately, by considering a plasma where the ions are fixed in space, over the time frame of interest, and the electrons obey a Maxwellian distribution such that the Boltzmann relation applies. Using Poisson's Equation in one dimension gives

$$\frac{d^2V}{dx^2} = -\frac{e}{\epsilon_0} (n_i - n_e) \quad (2.1)$$

where  $V$  is the electric potential and  $e$  is the electric charge. Since the ions are considered fixed, the density of ions will be constant and equal to the plasma density  $n_0$ . The Boltzmann relation then gives the electron distribution in the region of interest as

$$n_e = n_0 \exp\left(-\frac{eV}{KT_e}\right) \quad (2.2)$$

Substituting equation 2.2 into equation 2.1 gives

$$\frac{d^2V}{dx^2} = \frac{en_0}{\epsilon_0} \left[ \exp\left(-\frac{eV}{KT_e}\right) - 1 \right]. \quad (2.3)$$

To solve equation 2.3 the exponential can be expanded in a Taylor series, and neglecting terms of second order and higher gives

$$\frac{d^2V}{dx^2} = n_0 \frac{e^2 V}{\epsilon_0 K T_e} \quad (2.4)$$

The solution of equation 2.4 which is a homogenous second order linear ordinary differential equation is given by

$$V = V_0 \exp\left(-\frac{|x|}{\lambda_d}\right) \quad (2.5)$$

where,

$$\lambda_d = \sqrt{\left(\frac{\epsilon_0 K T_e}{n_0 e^2}\right)} \quad (2.6)$$

This quantity is known as the Debye length and is a measure of the thickness of the sheath that screens the bulk plasma from the effect of external fields. This screening applies as long as the dimensions of the bulk plasma is greater than the Debye length.

## 2. Sheath Effects

When a plasma comes in contact with a wall, the electrons and ions that hit the wall will recombine. But since the electrons are moving at a higher velocity than the ions, the electrons will be lost faster than the ions resulting in a net positive charge of the plasma. The wall will then be at a lower potential than the bulk plasma and an electric field will exist.

Figure 1 illustrates the potential variation in a plasma which is in contact with a wall. Due to Debye shielding a layer of charge separation, called the sheath, will exist. This layer will isolate the bulk plasma from the wall. The effect of the sheath is to accelerate the ions and to decelerate the electrons that enter the region until the flux of ions is balanced by the flux of electrons. Therefore, only those electrons in the high energy tail of the velocity distribution will be energetic enough to cross the sheath and others will be repelled back into the plasma.

The variation of the potential in the plasma sheath will now be considered. In order to simplify the problem, the following assumptions will be made:

1. The ions enter the sheath region with a drift velocity  $u_0$ , given by the Bohm criterion,
2. The ions have  $T_i = 0$  so that all ions have a velocity  $u_0$  at the plasma-sheath boundary,
3. The sheath region is collisionless and in steady state,
4. The potential decreases monotonically with  $x$ ,

5. The electrons follow the Boltzmann relation ( equation 2.2 ).

Applying conservation of energy to the ions in the sheath region gives

$$\frac{1}{2} Mu^2 = \frac{1}{2} Mu_0^2 - eV(x) \quad (2.7)$$

where  $V(x) < 0$ . Solving equation 2.7 for the ion velocity gives

$$u = \sqrt{u_0^2 - \frac{2eV}{M}} \quad (2.8)$$

The ion density within the sheath is determined from the ion equation of continuity which is given by

$$n_i(x)u(x) = n_0u_0 \quad (2.9)$$

Using equation 2.8 for the ion velocity, equation 2.9 can be solved for the ion density which gives

$$n_i(x) = n_0 \left(1 - \frac{2eV}{u_0^2 M}\right)^{-1/2} \quad (2.10)$$

Substituting equation 2.2 and 2.10 into equation 2.1 yields

$$\frac{d^2V}{dx^2} = \frac{en_0}{\epsilon_0} \left[ \exp\left(\frac{eV}{KT_e}\right) - \left(1 - \frac{2eV}{u_0^2 M}\right)^{-1/2} \right]. \quad (2.11)$$

This is the non-linear planar sheath equation. By multiplying each side by the first derivative of the potential, the equation can be integrated once to give

$$(V'^2 - V_e'^2) = \frac{2n_0KT_e}{\epsilon_0} \left\{ \left[ \exp\left(\frac{eV}{KT_e}\right) - 1 \right] + \frac{Mu_e^2}{KT_e} \left[ \left(1 - \frac{2eV}{Mu_e^2}\right)^{1/2} - 1 \right] \right\}. \quad (2.12)$$

Further solution of equation 2.12 would require numerical methods. If the electric field inside the plasma is zero, then the first derivative of the potential inside the plasma must also be zero. The left hand side of equation 2.12 is therefore greater than zero, and the following inequality results

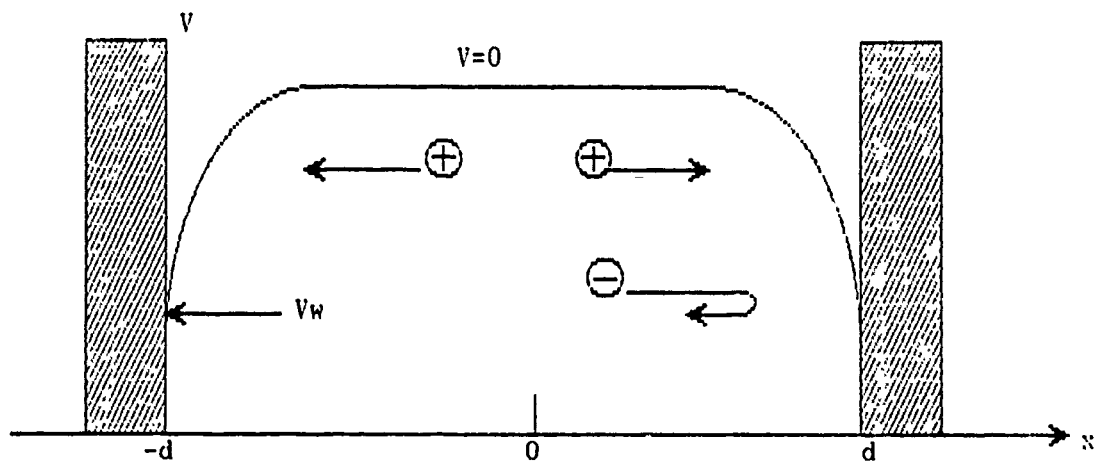


Figure 1. Plasma - Wall Interaction

$$\exp\left(\frac{eV}{KT_e}\right) - 1 + \frac{Mu_0^2}{KT_e} \left[ \left(1 - \frac{2eV}{Mu_0^2}\right)^{1/2} - 1 \right] > 0 \quad (2.13)$$

This inequality can be greatly simplified by expanding the left hand term in Taylor series and neglecting terms of third order and higher. The resulting inequality is known as the Bohm sheath criterion and is given by

$$u_0 > \sqrt{\frac{KT_e}{M}} \quad , \quad (2.14)$$

This requires that the ions must enter the sheath region with a velocity greater than the ion acoustic velocity of the plasma. In order for this to occur, there must be a finite electric field within the plasma. Therefore, the assumption that the potential and the electric field are zero at the plasma-sheath boundary is only an approximation [ Ref. 7].

### 3. Child - Langmuir Law

The current flow between the cathode and anode of a vacuum diode is limited by the space charge of the electrons that exist between them. The electrons distort the external field and thereby reduce and even reverse the field at the cathode surface.

As an example, consider a diode consisting of infinite flat plates a distance  $d$  apart. Assume that there is an unlimited supply of electrons available from the cathode, and that the initial velocity of the electrons after emission is negligible compared with the velocity that they will gain while crossing the electrode gap. The kinetic energy of the electrons crossing the gap and the current density carried by the electrons is given by

$$\frac{1}{2}mv^2 = eV \quad (2.15)$$

and

$$j = env \quad (2.16)$$

Using Poisson's equation, in one dimension, the current-voltage relationship can be derived as follows:

$$\frac{d^2V(x)}{dx^2} = \frac{en(x)}{\epsilon_0} \quad (2.17)$$

The electron velocity is determined from equation 2.15 to be

$$v(x) = \sqrt{\frac{2e}{m}} V^{1/2} \quad (2.18)$$

The electron density is determined using equation 2.16 and 2.18, and after substituting into equation 2.17 gives

$$\frac{d^2V}{dx^2} = \frac{j}{\epsilon_0} \sqrt{\frac{m}{2e}} V^{-1/2} \quad (2.19)$$

In order to solve equation 2.19 both sides are multiplied by the first derivative of the potential and reduced to the following form

$$\frac{d}{dx} \left( \frac{dV}{dx} \right)^2 = \frac{j}{\epsilon_0} \sqrt{\frac{2m}{e}} V^{-1/2} \frac{dV}{dx} \quad (2.20)$$

Equation 2.20 is then integrated over the gap using the boundary conditions that the electric field and the potential are zero at the cathode. The result of this integration gives

$$\frac{dV}{dx} = \sqrt{\left( \frac{2j}{\epsilon_0} \sqrt{\frac{2mV}{e}} \right)} \quad (2.21)$$

Integrating once again over the gap, applying the boundary conditions, and rearranging the desired current-voltage relationship yields

$$j = 4\sqrt{2} \frac{\epsilon_0}{9} \sqrt{\frac{e}{m}} \frac{V^{3/2}}{x^2} \quad (2.22)$$

Equation 2.22 is known as the Child-Langmuir law for space charge limited current flow [ Ref. 8]. Although it has been derived here using simple assumptions, the proportionality of the current density to the 3/2 power of the potential difference remains for more difficult geometries under non-relativistic conditions. It should also be pointed out that the Child-Langmuir law applies to both positive and negative charge carriers.

#### D. ELECTROSTATIC PROBE AND FARADAY - CUP MEASUREMENTS

The electrostatic probe has been used as a fundamental diagnostic tool for measuring plasma characteristics. The original use and theory was done by Langmuir (1924 - 1929). Hence, the electrostatic probes, particularly the single filament ones are called Langmuir probes.

The electrostatic probe basically consists of one or more small, metallic electrodes that are inserted into the plasma to be characterized. The electrodes may be cylindrical or spherical in shape, or may just be a plate or some other regular or irregular geometric shape which suits the probe surface area calculation model and does not interfere with the plasma flow.

The basic assumptions associated with electrostatic probe use are listed by Schott [ Ref. 9]:

1. The plasma to be infinite, homogeneous and quasineutral in the absence of the probe.
2. Electrons and ions have Maxwellian velocity distributions with temperatures  $T_e$  and  $T_i$ , respectively, with  $T_e \gg T_i$ .
3. Electron and ion mean free paths are much greater than the electrostatic probe radius for a cylindrical or spherically shaped probe.
4. Each charged particle hitting the probe to be absorbed and not to react with the probe material.
5. The region in front of the probe surface, where the plasma parameters deviate from their values in the undisturbed plasma to be confined to a space charge sheath with a well defined boundary. Outside of this boundary the space potential is assumed to be constant.
6. The sheath thickness  $d$  to be small compared to the lateral dimensions of the plane probe.

In the single probe configuration, the probe operates by a single electrode inserted into the plasma and attached to a variable power supply. The power supply can be biased at various potentials, positive or negative with respect to the plasma for optimal probe signal response. Current at the probe is measured as a function of the probe potential. The other electrode (using a plate or the wall of a metallic vacuum chamber) is a ground for the plasma.

The plate is normally fixed at a conducting section of the wall of the plasma confinement vessel. In electron discharge tubes the customary experimental arrangement uses the anode of the tubes as the reference electrode.

The theory of electrostatic probes is complicated because the probe electrodes are themselves plasma boundaries. At and near the plasma boundaries the plasma characteristics are changing, usually very markedly.

A thin layer called the Debye sheath exists at the boundary where electron and ion number density differ from the values within the plasma and electric fields are present.

The characteristic of Faraday-cup response is basically similar to a single probe characteristic. Separation of ions and electrons is done by static electric fields and the positive or negative current is collected in a Faraday cup. The Faraday cup signal was used to determine the time at which the laser produced plasma pulse arrived at the Faraday cup location. When a DC voltage is applied to the Faraday cup in a plasma, the ions are attracted by the negative electrode and the electrons by the positive one. A fundamental characteristic of the behavior of a plasma is its ability to shield itself from the electric field by forming a Debye sheath.

A detailed Faraday cup's detector schematic diagram is shown in Figure 5 (see Experimental Apparatus ).

The Faraday-cup was used to measure the ion density,  $n_i$ , using equation (2.16):

$$j = qn_i v_i \quad (2.16)$$

where ,  $j$  = current density =  $I/A$

$A$  = Faraday - cup hole area

$v_i$  = ion velocity =  $d/t$

$d$  = distance from the target to the Faraday - cup

$t$  = The time difference between the laser shot and the received signal (i.e., the time it takes the ions to travel from the target to the Faraday-cup )

One problem in this experiment is that the laser pulse is long, i.e., plasma is produced during the pulse duration.

### III. EXPERIMENTAL EQUIPMENT AND PROCEDURES

#### A. INTRODUCTION

This experiment was designed to determine the velocity and density of a  $CO_2$  laser produced plasma in a vacuum chamber. The laser energy was directed into the vacuum chamber via a beam splitter, mirrors, and a NaCl window. This required a variety of equipment which is described in the following sections.

#### B. EXPERIMENTAL APPARATUS

##### 1. Laser

The Lumonics TE-822 HP  $CO_2$  high energy TEA pulsed (Figure 2 on page 15) laser was utilized to irradiate all targets. This laser's active medium consists of a continually flowing gas mixture of He,  $N_2$  and  $CO_2$ . In the single pulses mode, it is capable of delivering a maximum of 20 joules of output with an adjustable pulse width of 0.05 microseconds to 5.0 microseconds. In the multiple pulse mode, the laser is capable of delivering a maximum of 8 joules per pulse. The laser's nonregulated high voltage power supplies were cooled by an external water refrigeration unit and controlled by a voltage regulator. The formal laser operating procedure is documented in a manual [ Ref. 10].

##### 2. Vacuum System

The VEECO 400 vacuum system ( Figure 3 on page 16) is utilized in conjunction with the  $CO_2$  laser for research of plasma surface interactions at the Naval Postgraduate School. The vacuum pumping system consists of a mechanical pump, a water cooled diffusion pump, and a liquid  $N_2$  cooled cold trap. The pressure range of the chamber is from 1.0 atmosphere down to  $10^{-9}$  atmospheres (atm ). The mechanical pump was used to reduce the background pressure to 1.0

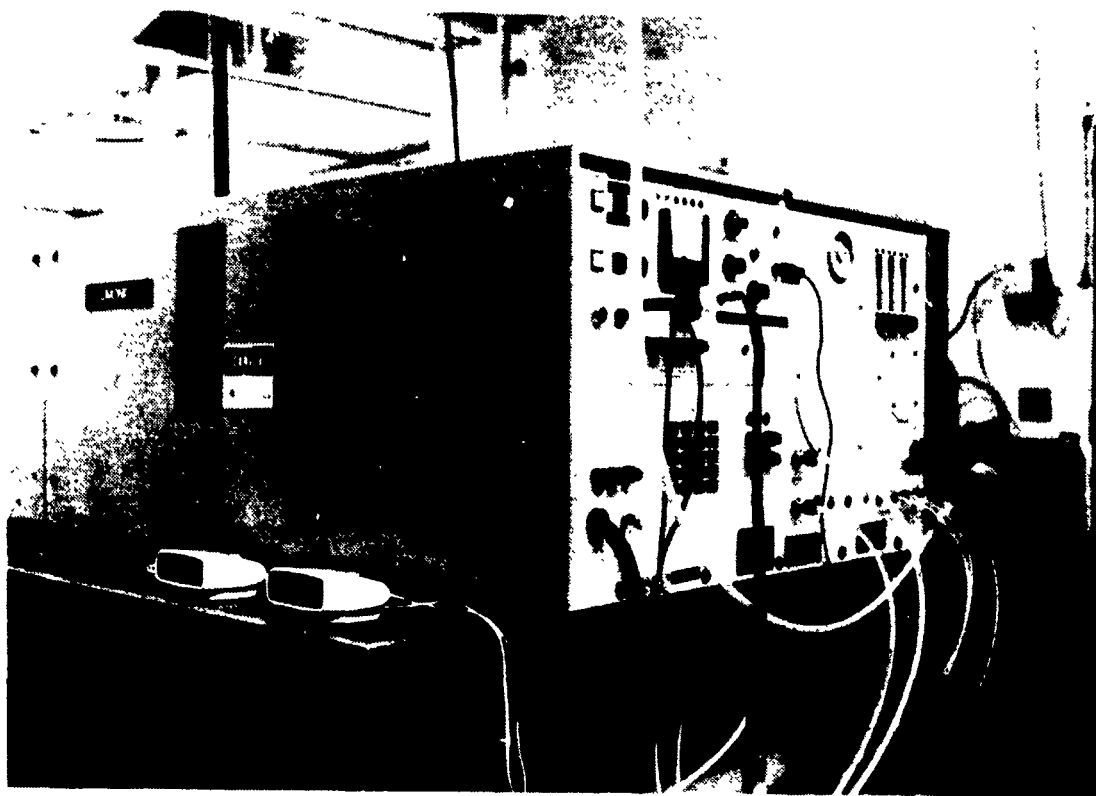


**Figure 2. Lumonics TE-822 HP CO<sub>2</sub> Laser**

mTorr, the background pressure was further reduced by the diffusion pump. Three different gauges are required to determine the pressure in different ranges. Pressure between 760 Torr and 10 Torr were monitored on the Matheson pressure gauge (model 63-5601) mounted on top of the chamber [Ref. 11]. Pressure between 10 Torr and 1.0 mTorr were monitored on the Granville- Phillips service 275 pressure gauge also located on top of the chamber. Pressures below 1.0 mTorr were obtained from an ionization gauge located below the chamber just above the diffusion pump. This gauge is a fixed component of the VEECO 400 system.

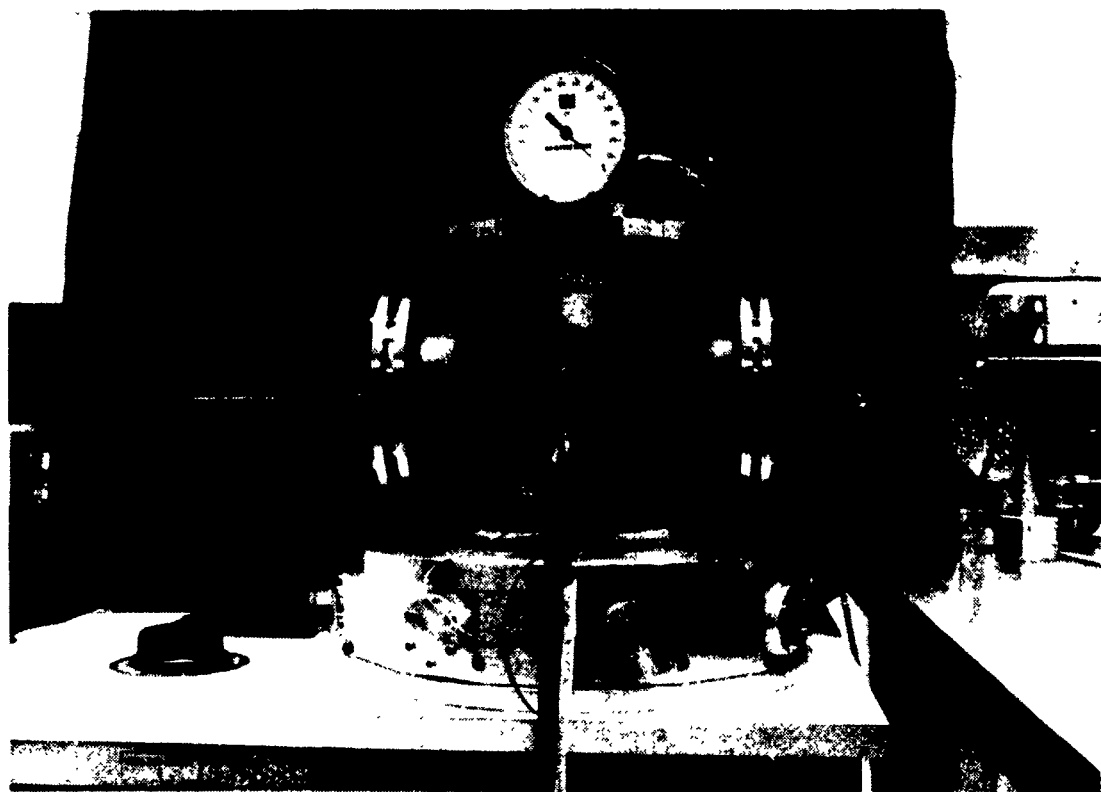


**Figure 3. VEECO 400 Vacuum System**

### **3. Optics**

The optics consisted of a beam splitter, focusing lens, and an optical window for allowing the laser beam to enter the vacuum chamber. The specific characteristics of each component are listed below :

- \* One 7.62 cm diameter ZnSe beam splitter with 99.38 % reflectance, and 0.13% transmittance.
- \* One 7.62 cm diameter ZnSe focusing lens with 98.5 % transmittance, and 38 cm focal length.
- \* One 7.62 cm diameter NaCl window with 92 % transmittance.

This combination provided a 90.1 % transmission factor of the total beam energy into the vacuum chamber.

#### **4. Energy Meter**

The energy output of the laser was measured using the laser precision corporation model Rj-7100 energy meter with the model Rjp-736 energy probe which is designed to detect laser pulses of wave lengths between 0.35 and 11.0 microns ( Figure 4 on page 18). The meter is capable of measuring the energy of a laser pulse of 1 nsec to 1 msec duration, and total energy ranging from 10  $\mu$ J to 10 J [ Ref. 12]. The energy detected at the probe is only a small percentage (0.13 % ) of the total energy of the laser pulse, whose flux on the target is calculated from the reflectance and transmittance of the ZnSe beam splitter, as well as the transmittances of the ZnSe focusing lens and NaCl window.

#### **5. Oscilloscope**

Faraday-cup signals were recorded using the Tektronix 7844 dual beam oscilloscope and C-50/C-70 series cameras. The laser " sync-out " was used throughout the experiment as the oscilloscope triggering input. The C-50/C-70 camera was operated manually to ensure the single sweep traces were recorded. This also afforded the opportunity to use double exposures to record different signal inputs. An attempt was also made to use the Tektronix 7844 dual beam oscilloscope to record two different Faraday-cup signals.

#### **6. Detector Assembly**

Figures 5 and 6 depict the Faraday cup detector and circuit used throughout this experiment. The Faraday cup cover was made of brass tube. The cup detector was connected with a 90 degree bend to the BNC. An entrance aperture smaller than the detector diameter is used to define the entrance plasma diameter. The cup was electrically insulated with nylon strips at the end of the detector. The charge collector cup registers time resolved signals of ion and

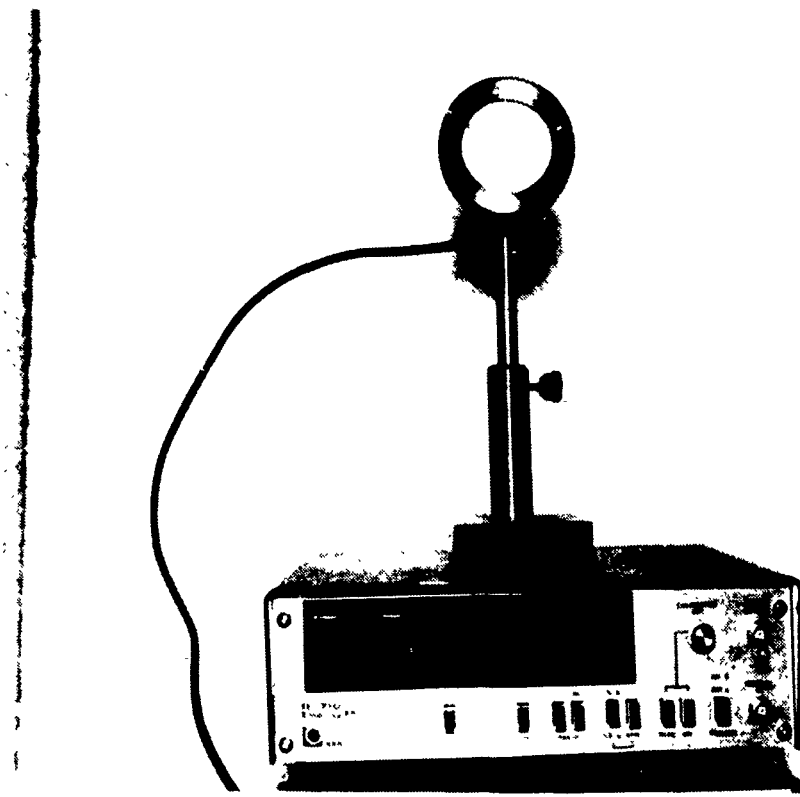


Figure 4. RJ-7000 Energy Meter and RJP-700 Probe

electron arrivals. The time scale for such collection is less than the  $2\mu s$  detector circuit response time. The voltage to the Faraday cup is supplied through a current limiting  $50\ \Omega$  resistor.

In this experiment, two kinds of Faraday cup covers, detectors and connecting methods were used. One cover has one hole drilled at the center of the cover with a diameter of 0.651 mm and an area of  $0.33mm^2$ , while the other has four small holes with a diameter of 0.353 mm each and a total area of  $0.39mm^2$ , as shown in Figure 7. Both different Faraday cup covers were used to determine the parameters of the plasma flow. The cover with four small holes resulted in less plasma entering that cup than the cup with one hole. This experiment was conducted to study the change of the I-V characteristic as a function of entrance

area. If a relatively large plasma stream enters through the hole in the cover and into the cup, the I-V characteristic will be similar to the one of double probe.

In previous experiments by F. Schwirzke at the Kernforschungszentrum, Karlsruhe, Germany, using Faraday cups to diagnose a streaming carbon plasma produced by plasma guns it was observed that the current showed sharp spikes. Figure 8 compares two Faraday cup signals at a bias voltage of -25 V. FC 3 on channel 2, CH2, has a 0.5 mm diameter entrance hole while FC 1 on Channel 1, CH1, has a smaller hole diameter of 0.3 mm. These current spikes can be explained by a spark discharge inside the Faraday cup between the cup and the cover. The electric field inside the Faraday cup depends on the bias voltage and the separation distance between cup and cover. Sharp corner of the cup will enhance spark formation.

To observe how sparking depends on the pressure and distance, two differently shaped detectors were used. One with thick walled and with sharp corners and the other one thin and with round corners as shown in Figure 9.

During the course of this experiment it was observed that two Faraday cup with different connections of the detector to the BNC cable gave different results. Figure 10 shows that one detector was mechanically joined to the inner hollow conductor of the coax cable (called normal) while the other one was soldered to the cable.

## 7. Experimental Set - Up

The arrangement of the equipment for this experiment was almost identical in all respects, to the previous experiments performed by Henson [ Ref. 13], except for the use of Faraday cups. The output beam of the Lumonics Laser is directed onto the ZnSe beam splitter located in the beam path as shown in Figure 11. The radiation transmitted through the beam splitter is incident on the the DMSL IR detector.

The reflected beam is passed through the ZnSe focusing lens and NaCl window into the vacuum chamber, and onto the target. Inside the chamber, the Faraday cup was located in several locations during various phases of the experiment. The primary locations,  $L_1$ , were at distances of 5 cm, 10 cm, 15 cm, on a line 30 degrees off the target normal. A second location,  $L_2$ , was opposite the target on a line  $26 \pm 3$  degrees off the target, and at a distance of  $18\text{cm} \sim 20\text{cm}$  from the target as shown in figure 11. These different locations provided a means for evaluating the effects of plasma expansion on the signals detected.

The target was held in a fixture inside the vacuum chamber at a distance of 13.6" from the lens.

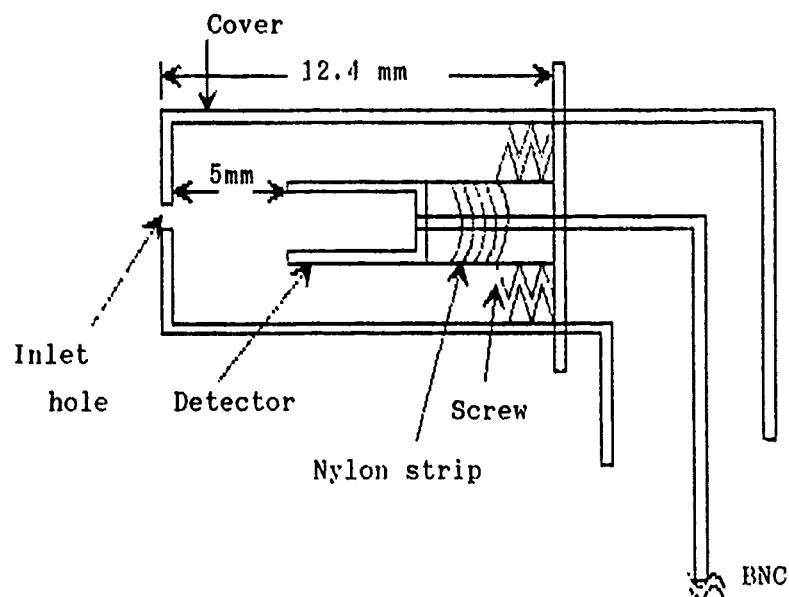


Figure 5. Faraday Cup Schematic

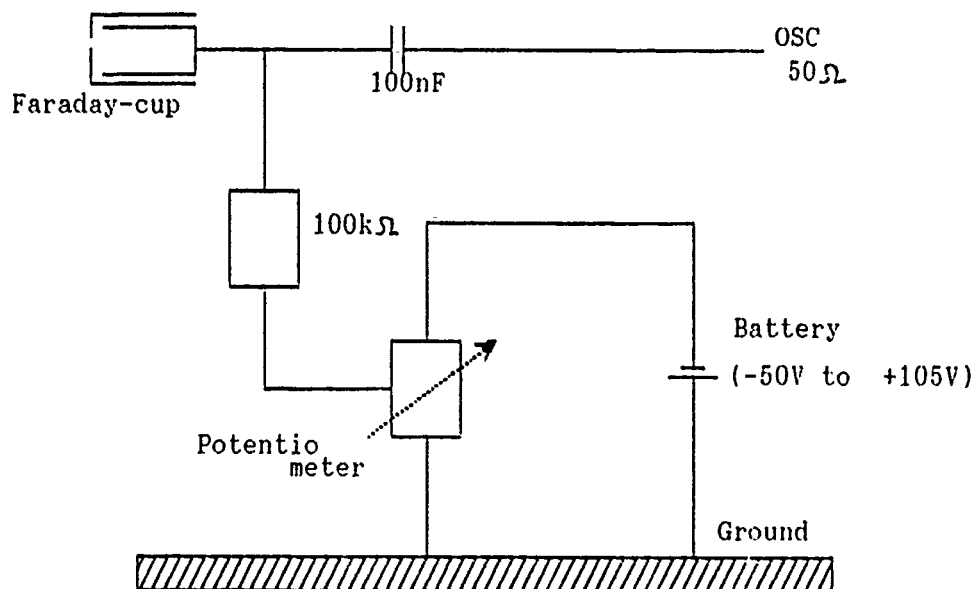


Figure 6. Circuit Schematic

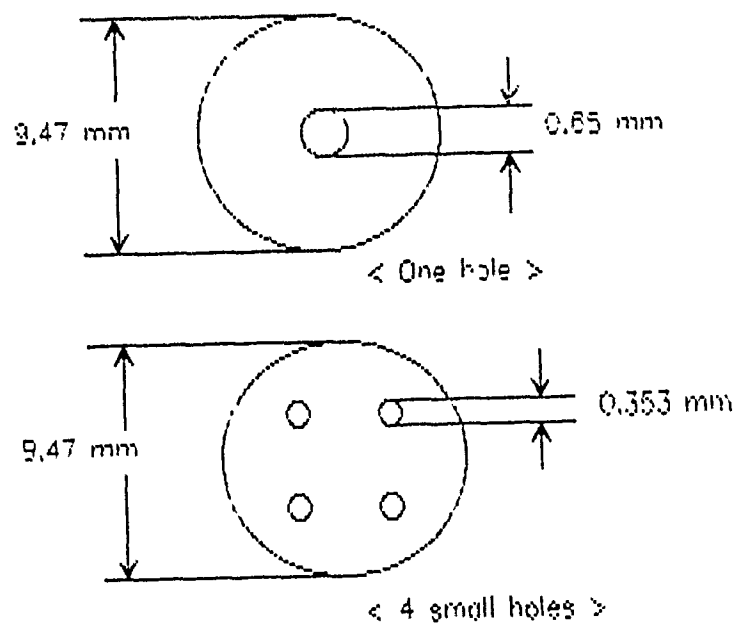


Figure 7. Faraday Cup Cover Hole, Schematic

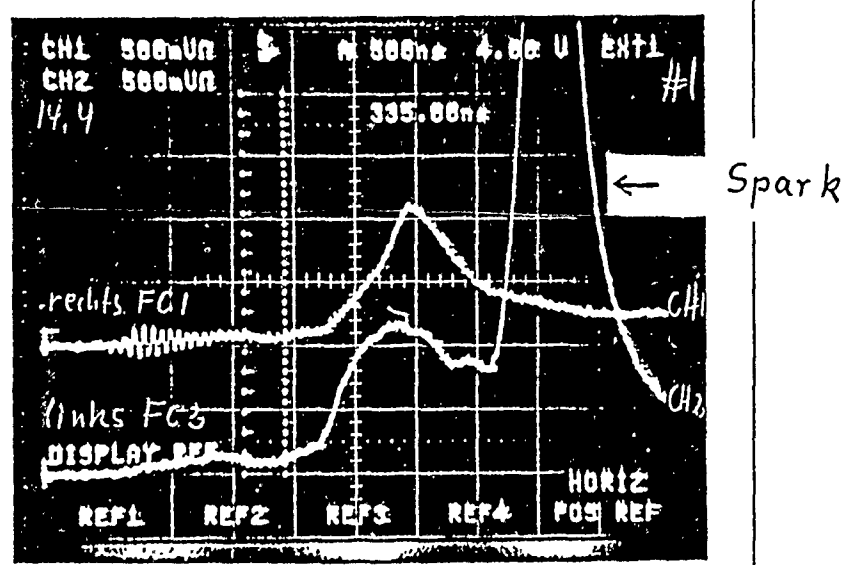
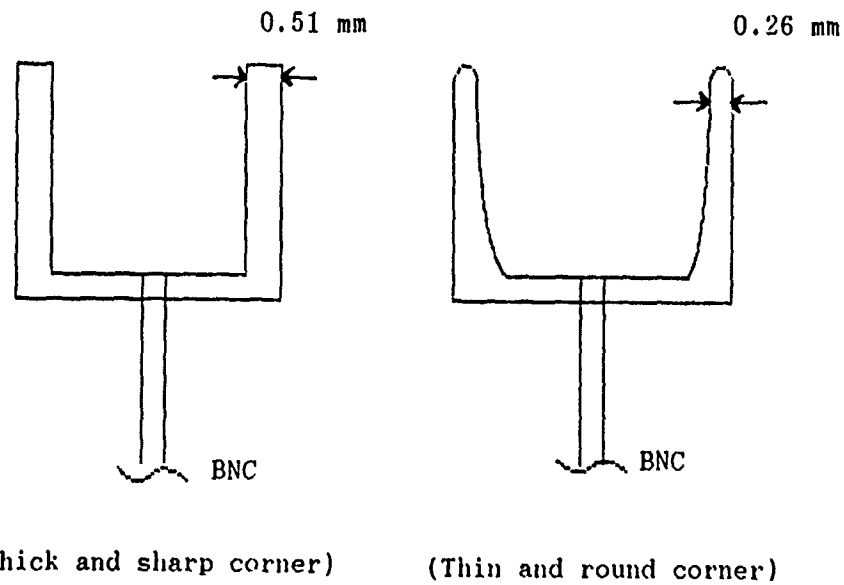


Figure 8. Comparison of Current Signals of Two Faraday Cups FC1 with 0.3 mm Entrance Hole and FC3 with 0.5 mm Hole. Bias V = -25 Volt



**Figure 9.** Two Kinds of Detector Rim, Schematic

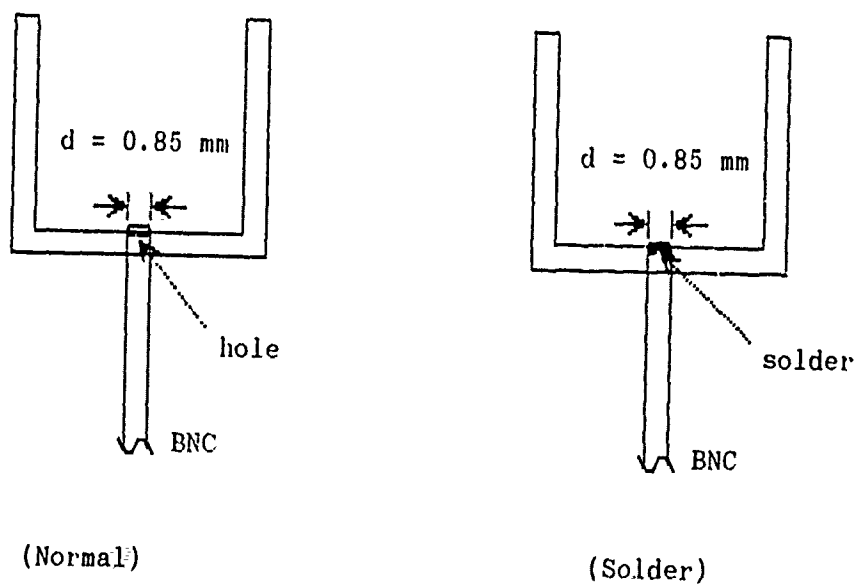


Figure 10. Different Methods of Connection of Detector to BNC Cable

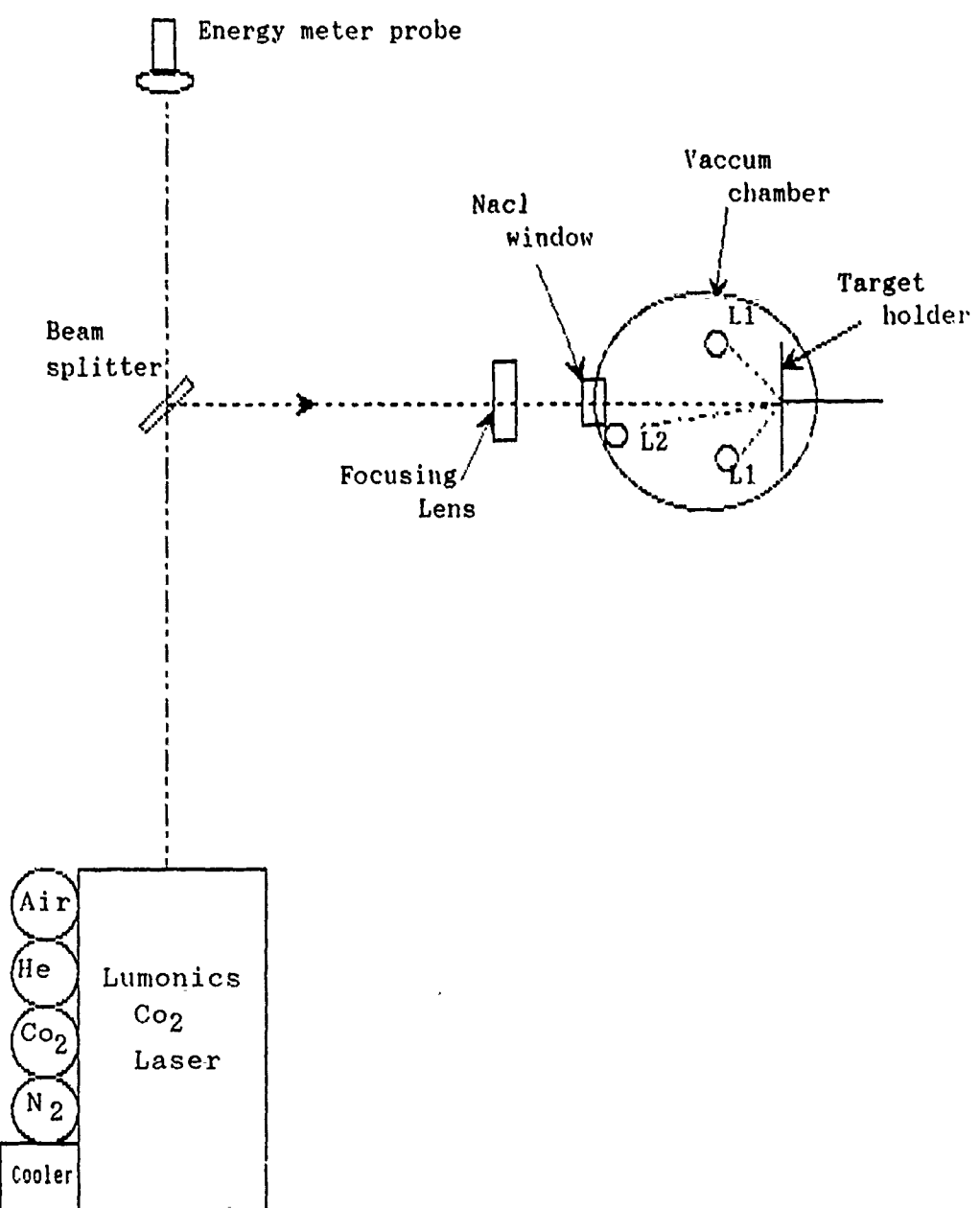


Figure 11. Configuration of Equipment

## C. EXPERIMENTAL PROCEDURE

### 1. Target Description and Preparation

Lexan, a polycarbonate manufactured by General Electric, was used as the target material due to its ease of preparation for use. Lexan target preparation consisted of cutting approximately 6.87 cm rectangular plates of the 3mm thick material, rinsing it with reagent grade ethyl alcohol, and blow drying it prior to mounting in the vacuum chamber.

These rectangular plates were placed flat against the target holder, and rotated between shots in order to provide a new target area clear of damage from the previous laser shot.

### 2. Energy Measurements

Laser energy readings were recorded for all shots. This included 480 shots at the 25 KV capacitor potential. Over the course of the experiment, the average energy at the 25 KV potential was found to be  $11.82 \pm 0.84$  J. During any run, the energy readings never varied by more than 10 %, and were generally less than 5 %.

### 3. Faraday Cup Signal Measurements

Electron and ion current signals were detected by the Faraday cup and displayed on the Tektronix 7844 dual beam oscilloscope. Signal traces were recorded on polaroid 47 and 667 film for evaluation and comparison. Variables in the investigation included detector location and cup bias voltage.

Once mounted on the target wheel, the targets were placed in the vacuum chamber, the chamber sealed and evacuated to  $10^{-5}$  Torr. The energy was adjusted by placing a plexiglass stopper before the vacuum chamber and firing the

laser while adjusting the capacitor voltage. Once the beam energy was adjusted, the stopper was removed, the lab darkened, and the laser shot made.

Plasma formation was determined by observing the laser-target interaction with a polaroid camera. If there was light emitted from the surface, plasma was formed. Most of the data were recorded using type 47 rol film. The camera shutter was held open by a remote cable release for approximately 3 second before and after the shot.

The observed Faraday cup signal was caused by generation of the plasma and its expansion away from the target surface. Therefore, a series of experimental shots were performed to determine to what extent the cup bias voltage influenced the current reading. Signals were recorded at select locations  $L_1$  and  $L_2$  for different cup bias voltages.

## IV. EXPERIMENTAL RESULTS

The experimental results of the research completed for this thesis are presented in this section. Each aspect of the results has been subdivided into several subsections for easy identification. The data collected during this experiment consisted exclusively of oscilloscope trace photographs. Determination of signal amplitude and time are derived directly from these traces.

### A. MEASUREMENT ON LASER PRODUCED PLASMA

#### 1. Ionization and Sparking in An Electric Field

When an electron or a positive ion moves through a gas which does not form negative ions, it is likely to excite or ionize atoms or molecules by collisions provided its energy exceeds the corresponding critical values. In the presence of an electric field, however, excited atoms as well as new electrons and ions are found throughout the gas together with the primary particle; they may be distributed over a region which is bounded by the electrodes and the walls confining the space. If the voltage is high enough between the cover and the detector and sufficient gas is trapped in the cup then breakdown can occur within the Faraday cup.

In order to find the breakdown field or sparking voltage in terms of the gas pressure, and the electrode distance, equation (4.1) [ Ref. 14] can be used

$$\frac{V}{pd} = \frac{E}{p} \quad (4.1)$$

where  $V$  : Sparking Potential (volts)

$p$  : pressure

$d$  : discharge gap with two plane electrodes.

Normally, from the Paschen curve the minimum sparking potential for air is  $V_{\min} = 330$  (volts) at  $pd = 0.57$  mmHg cm. Therefore,  $V/pd = 579$  V/cm mmHg as shown in Figure 12 [Ref. 14]. In this experiment, the calculated Faraday cup sparking potential becomes, using equation (4.1),  $V/d = 20$  V/0.5 cm = 40 V/cm. If the vacuum pressure is approximately  $10^{-5}$  mmHg, then  $Pd = 0.5 \times 10^{-5}$  mmHg cm and the breakdown voltage would be very large. However, the pressure may increase in the Faraday cup when the plasma enters because its contact with the inside surface leads to desorption of gas which is only slowly pumped through the small hole in the cover of the Faraday cup. The required pressure for the Paschen minimum would be  $P = \frac{V}{d(579)} = \frac{40}{579} = 0.07$  mmHg, a value which can exist inside due to desorption.

Two kinds of Faraday cup's rim were used. One is sharper and thicker than the other. Figures 13 and 14 shows the Faraday cup current as function of time, at a distance of 10 cm from target, bias potential -20V, and shape of cup rim.

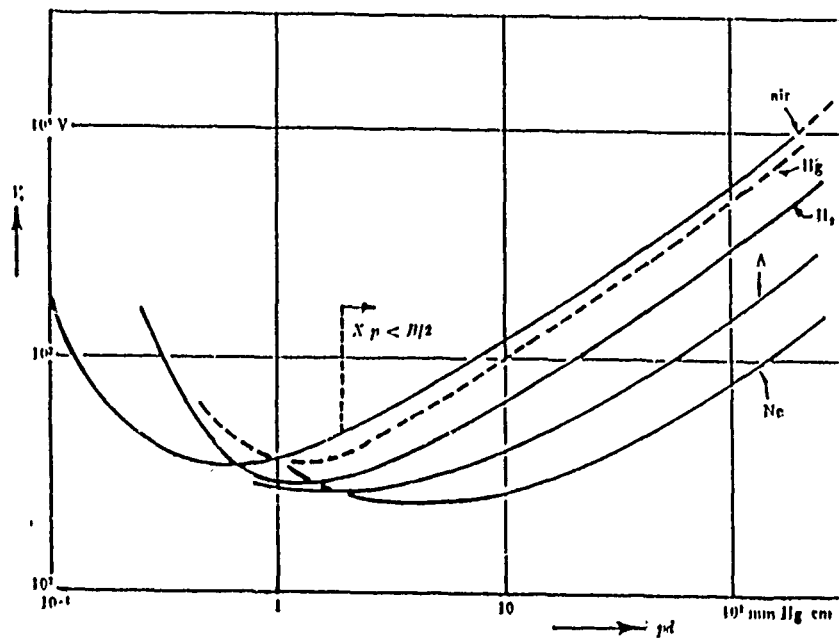


Figure 12. Sparking Potential (V) as a Function of The Reduced Electrode Distance Pd in Several Gases [Ref.14]

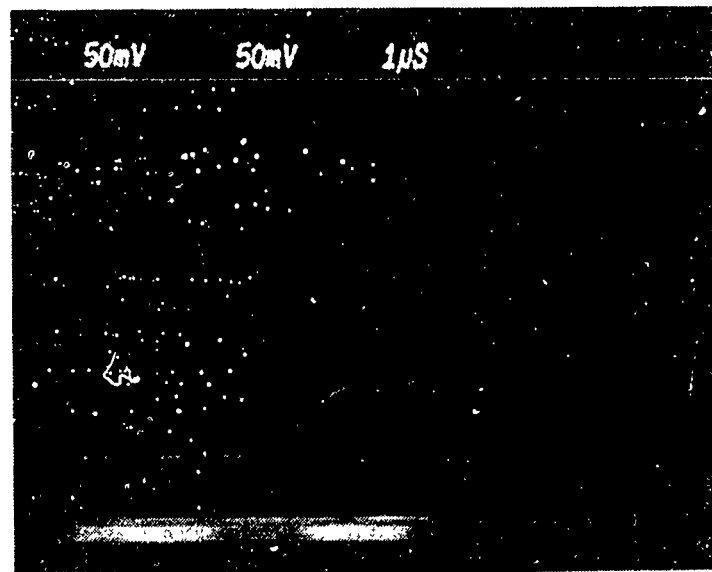


Figure 13. Distance 10 cm, Potential -20 V in Thin and Round Edge Faraday Cup

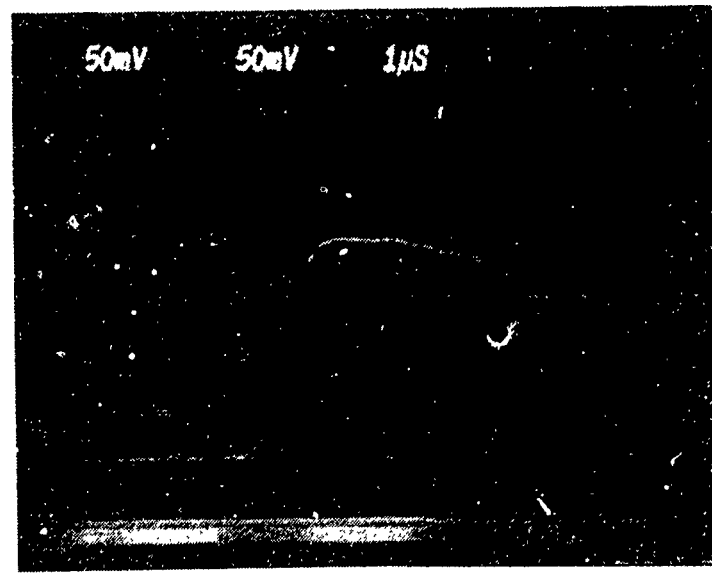


Figure 14. Distance 10 cm, Potential -20 V in Thick and Sharp Edge Faraday Cup

## 2. Response Signal as Function of Distances

By varying the distance to 5 cm, 10 cm, 15 cm, 20 cm, from the target we observed that close to the target the electron and ion current increased linearly with positive or negative cup bias voltage (see figure 15). This result is similiar to a double probe characteristic. If the Debye length is larger than the diameter of cover hole, then , an equal electron and ion current would be drawn to the cup and cover if a bias voltage is applied. At a larger distance from the target and thus lower plasma density, the ion current curve tends to saturate like a single probe characteristic. The reason for this is that, if the cover hole radius becomes smaller then the Debye length, then the electrons will be turned away by the positively biased cup. This effect is shown in Figure 15.

One hole and four small hole covers were tested at the same distance of 20 cm. When using the four small hole cover, it resulted in a curve approuaching a single probe characteristic. (i.e.,small ion saturation current)

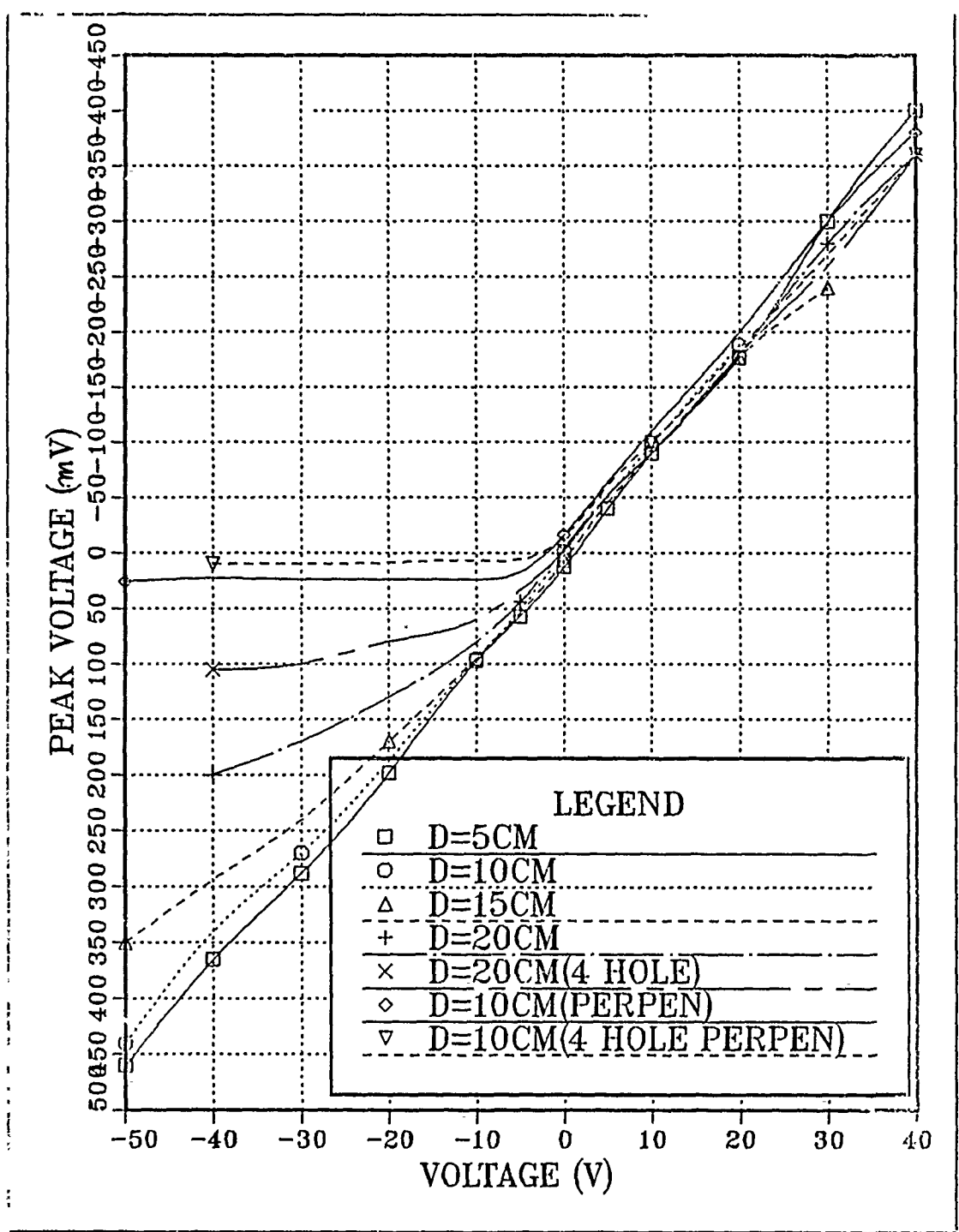


Figure 15. Peak Voltage vs Bias Voltage at Variable Distance ( Normal Faraday Cup)

### 3. Measurements Parallel and Perpendicular to Streaming Plasma

The transition from double to single probe characteristic was very pronounced when the Faraday cup was aligned perpendicular to the plasma flow. The parallel orientation of Faraday cup is shown in Figure 16 on page 32. The directed ion flow (and electrons) enter into the detector with equal flow rates. The ion and electron branch of the characteristic are almost the same, as shown in Figures 17 through 21 on page 33-35. This is similar to a double probe characteristic.

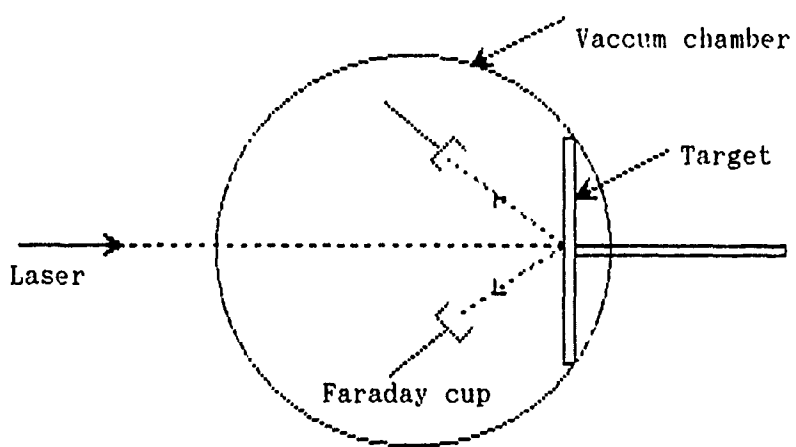


Figure 16. Parallel Orientation of Faraday Cup

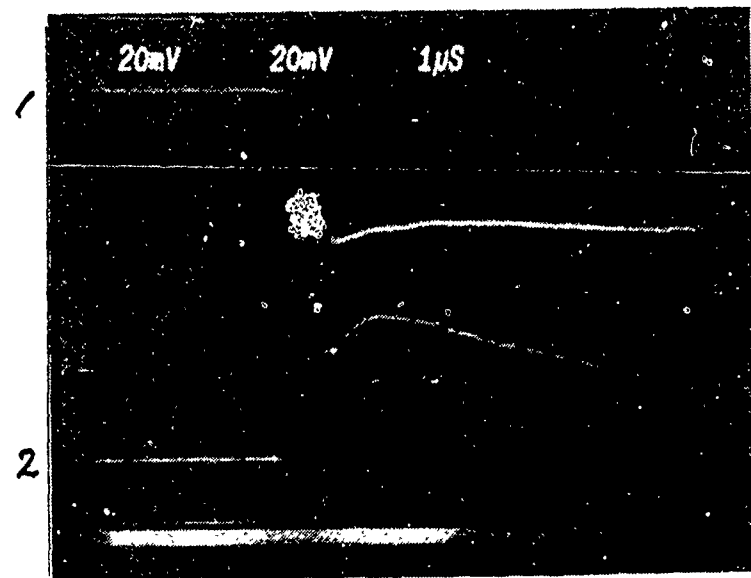


Figure 17. Peak Voltage vs Time at  $\pm 5V$  Probe Voltage in Parallel Orientation  
(1-Electron Current, 2-Ion Current)

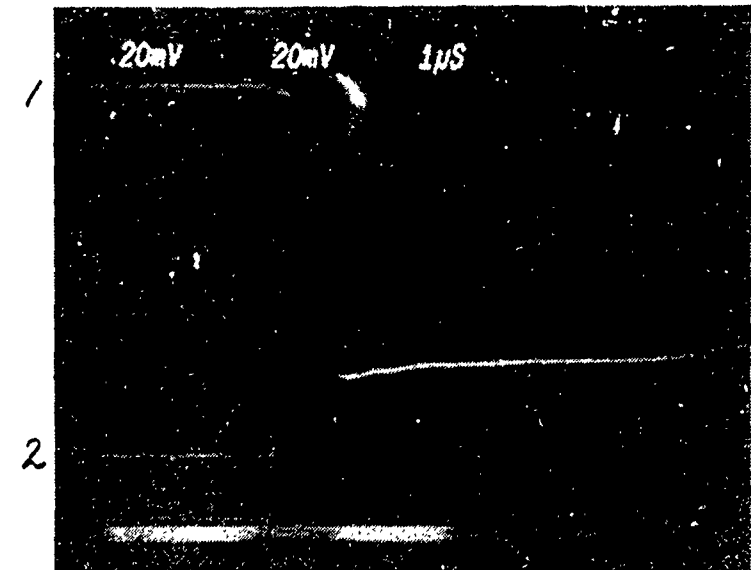


Figure 18. Peak Voltage vs Time at  $\pm 10V$  Probe Voltage in Parallel Orientation  
(1-Electron Current, 2-Ion Current)

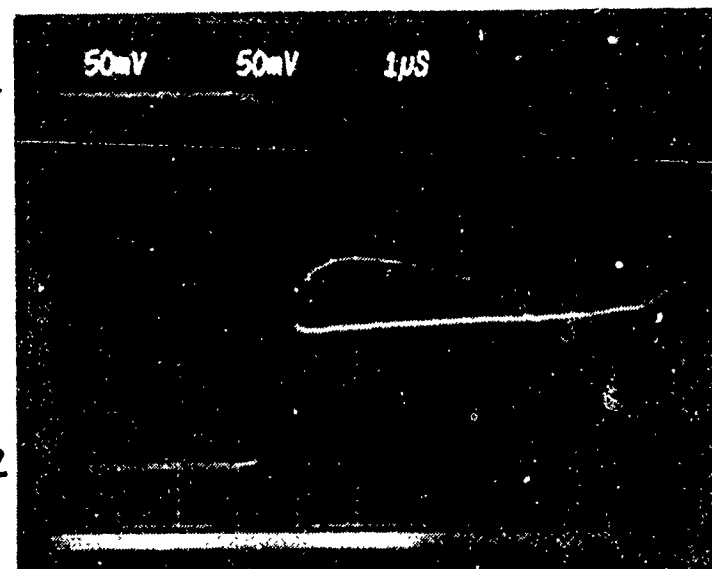


Figure 19. Peak Voltage vs Time at  $\pm 20V$  Probe Voltage in Parallel Orientation  
(1-Electron Current, 2-Ion Current)

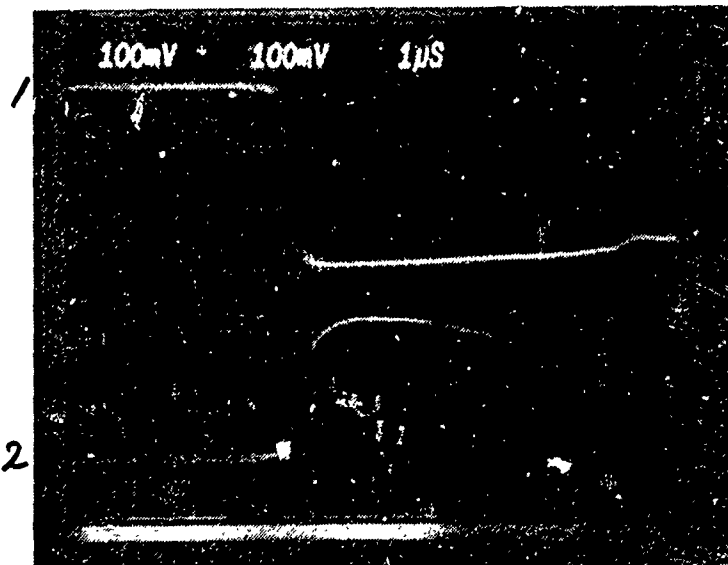


Figure 20. Peak Voltage vs Time at  $\pm 30V$  Probe Voltage in Parallel Orientation  
(1-Electron Current, 2-Ion Current)

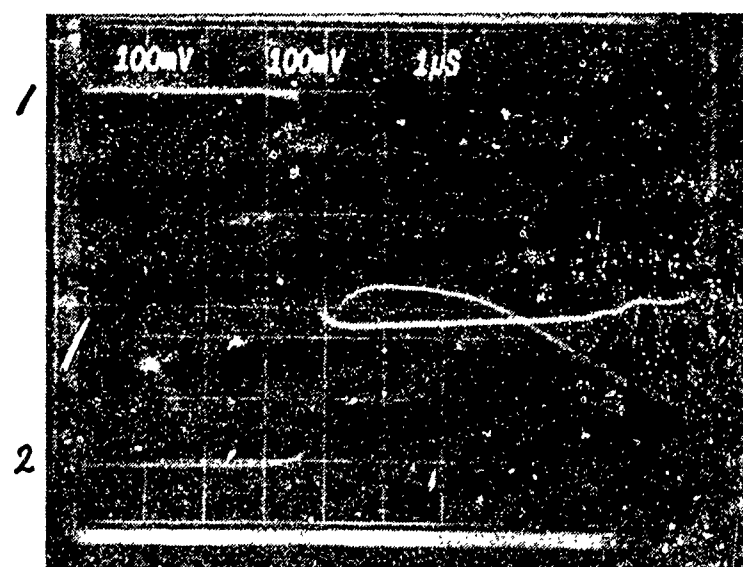


Figure 21. Peak Voltage vs Time at  $\pm 40V$  Probe Voltage in Parallel Orientation  
(1-Electron Current, 2-Ion Current)

The second case was the perpendicular orientation of the Faraday cup as shown in Figure 22 on page 36. Electron current amplitude was the same as in the parallel position, but the ion current is reduced in amplitude. The ion current is given by the ion flux perpendicular to the direction of flow, Figures 23 through 27 on pages 37-39.

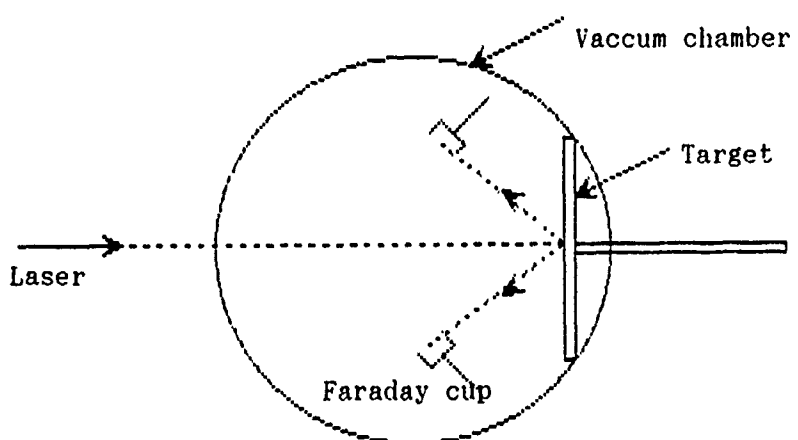


Figure 22. Perpendicular Orientation of Faraday Cup

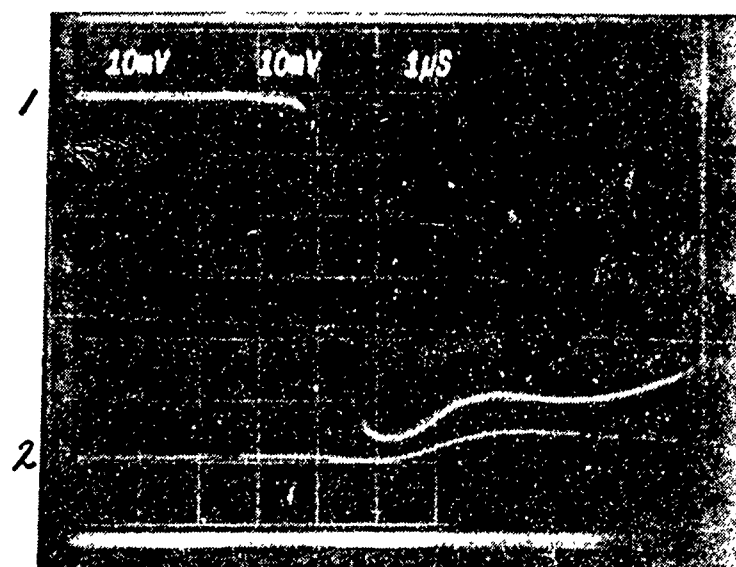


Figure 23. Peak Voltage vs Time at  $\pm 5V$  Probe Voltage in Perpendicular Orientation (1-Electron Current, 2-Ion Current)

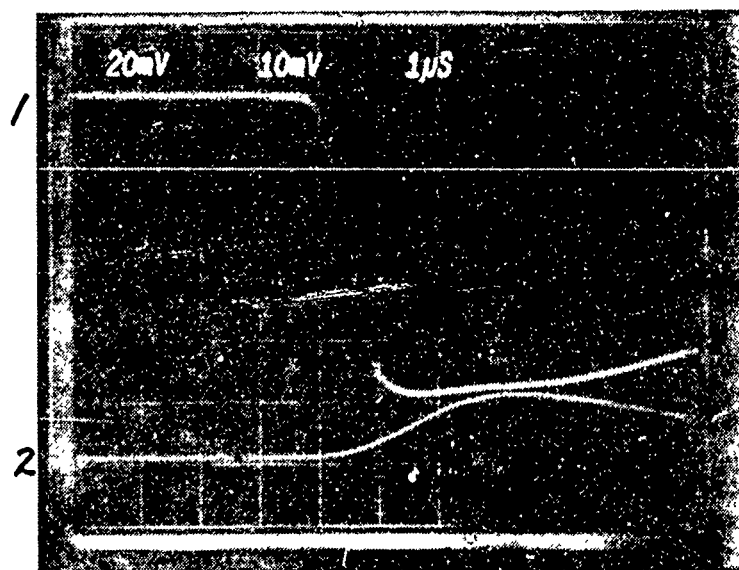


Figure 24. Peak Voltage vs Time at  $\pm 10V$  Probe Voltage in Perpendicular Orientation (1-Electron Current, 2-Ion Current)

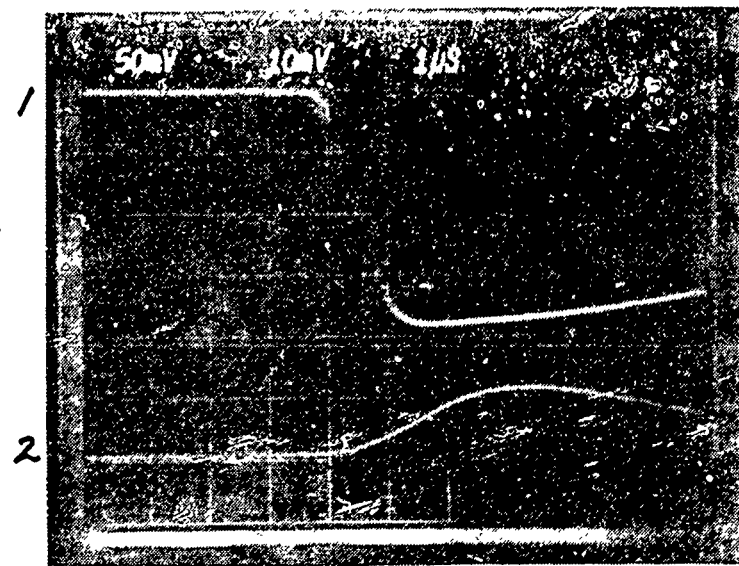


Figure 25. Peak Voltage vs Time at  $\pm 20V$  Probe Voltage in Perpendicular Orientation (1-Electron Current, 2-Ion Current)

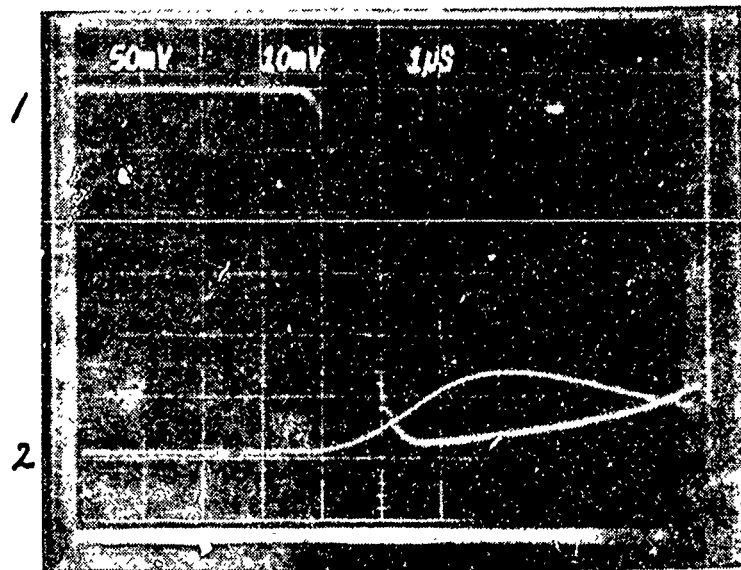


Figure 26. Peak Voltage vs Time at  $\pm 30V$  Probe Voltage in Perpendicular Orientation (1-Electron Current, 2-Ion Current)

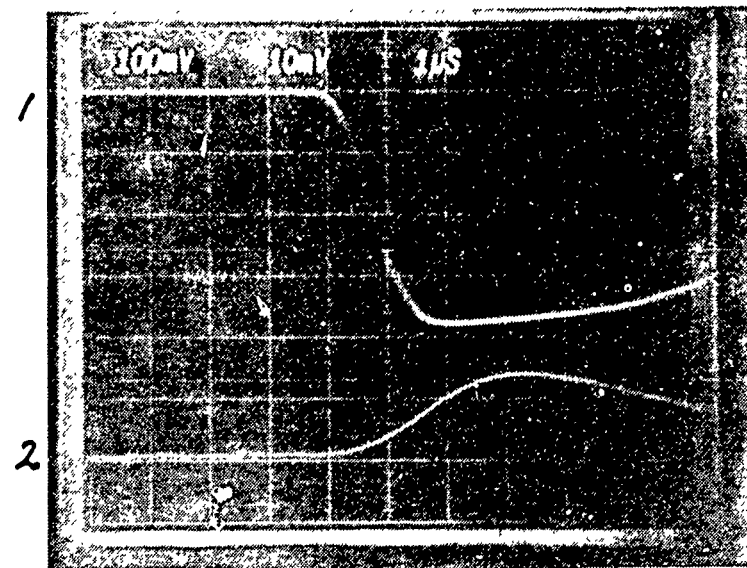


Figure 27. Peak Voltage vs Time at  $\pm 40V$  Probe Voltage in Perpendicular Orientation (1-Electron Current, 2-Ion Current)

#### 4. Difference of Signals between Various Detectors

In Figure 15 and 28, the ion and electron currents are plotted for two different Faraday cup detectors. The soldered and normal connected cups did not vary much in the electron current. However, the soldered detector showed a reduced ion current compared to the normal detector. It is unknown if this is just a fluctuation in the measurement or if the soldered surface has an influence on the ion measurement, for example by changing the secondary electron emission coefficient.

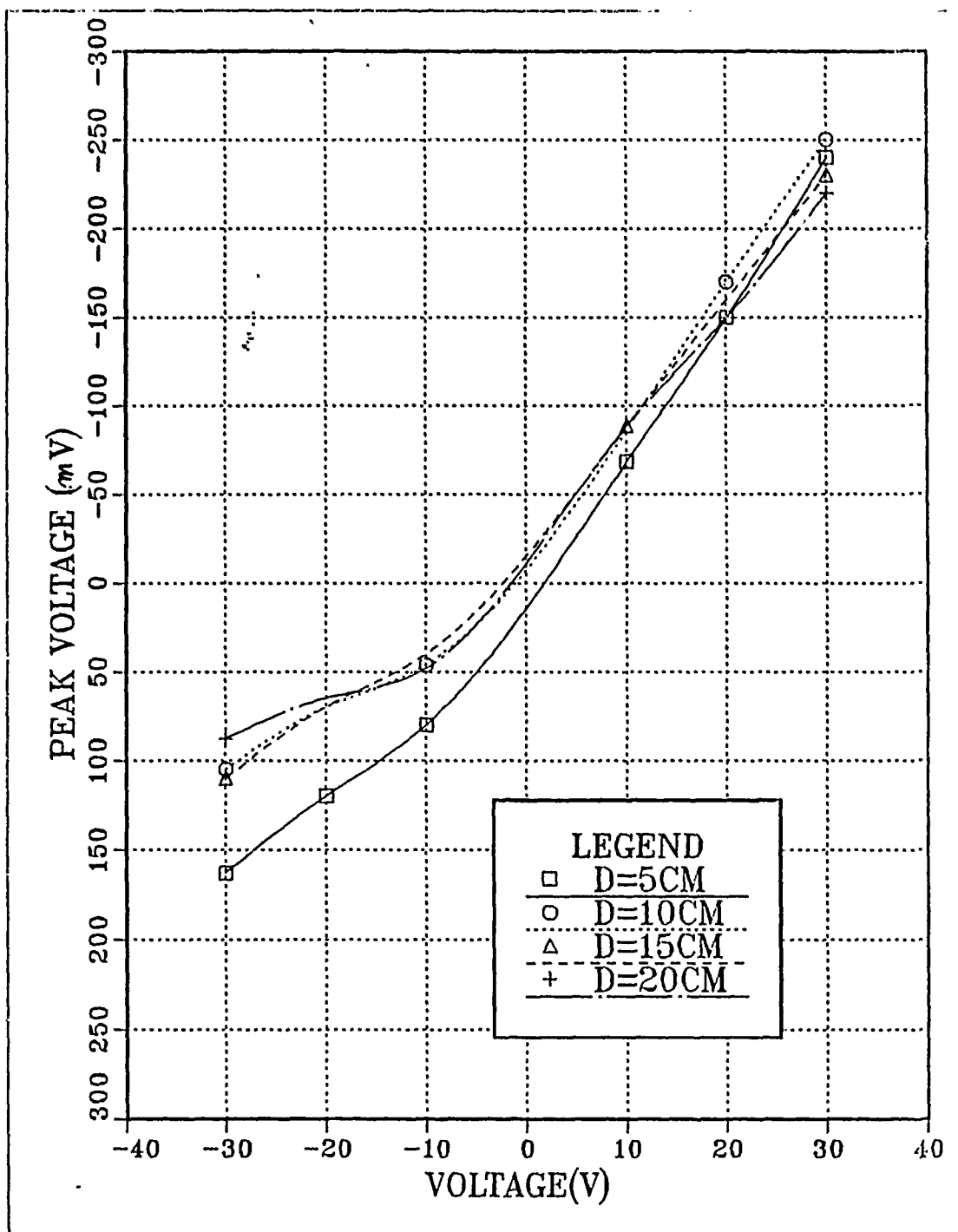


Figure 28. Peak Voltage vs Bias Voltage at Variable Distance (Soldered Faraday Cup )

## B. EVALUATION OF PLASMA PARAMETERS

The numeric values calculated in the following paragraphs are referred to throughout the text, but are presented in this chapter for ease of reference to the figures from which they are derived.

### 1. Plasma Expansion Velocity

The expansion velocity of a laser-produced plasma from an Lexan target was investigated. The target was suspended in a vacuum chamber at a pressure of  $4.8 \times 10^{-5}$  to  $2.2 \times 10^{-5}$  Torr. A ruler is used to measure the distance of the probe from the surface of the target. 2 Faraday cups were placed along the same line of plasma expansion with a distance gap of 5cm or 10cm between them.

To be able to consistently record the signals in the same time reference, a zero time mark,  $t_0$ , had to be displayed on each photograph. It was determined that it was desirable to compare the signal peak values for different values of probe bias. A linear time to distance relationship was assumed and calculations were made on the basis of this assumption, i.e.  $d = vt$ , where  $d$  is the distance the plasma had to travel and  $t$  is the time of the plasma arrival at the cup.

Error analysis of the calculations of velocity and distance was also necessary to insure that the measured quantities were dependable. A simple scheme for error analysis found in reference was used [ Ref. 15]. The measurement errors for distance  $d$  were  $d = \pm 0.05\text{cm}$ .

In this experiment the velocity was calculated from two measurements, one with parallel orientation, the other with perpendicular orientation of the Faraday cup. For parallel orientation, the ion velocity was calculated from Figures 29, 30 on pages 45. Electron velocities were calculated from Figures 31 and 32. From these calculations follow that, ions and electrons arrive at the same time. For the maximum of the signal the velocity is

$$v = \frac{10}{0.8 \times 10^{-6}} = 1.25 \times 10^7 \text{ cm/sec}$$

The velocity was also calculated with the perpendicular orientation of the Faraday cup. Electron velocity was calculated from Figures 33 and 34 on page 47. The figures show, an electron arrival time of  $t = 0.8 \mu\text{sec}$  as in the parallel orientation, therefore,  $v = 1.25 \times 10^7 \text{ cm/sec}$ .

## 2. Measurement of Electron Temperature

Electron plasma temperature can be found from the slope of the electrostatic probe characteristics, using the following equation (4.1)

$$\frac{d \ln I_e}{d V_p} = \frac{e}{K T_e} \quad (4.1)$$

For electrostatic probe diagnostics see Chen [ Ref. 16]

The measured value of

$$\frac{d \ln I_e}{d V_p} = \frac{1}{2.4} (\text{Volt})^{-1}$$

was derived by extrapolation of the graph in Figure 35 from the normal and 4 small hole curves. The plasma electron temperature is approximately 2.4 eV at a distance 10 cm from the target surface.

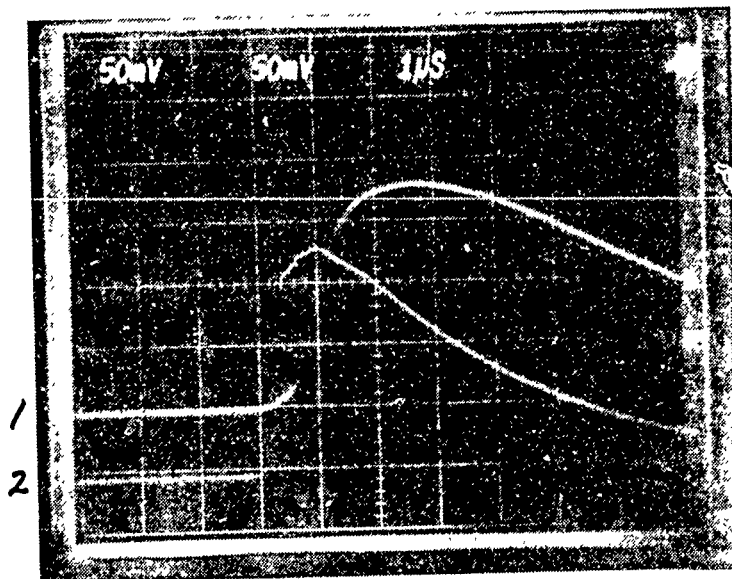


Figure 29. Distance Gap 5 cm, Probe Bias Voltage -20 V, in Parallel Orientation  
(Faraday Cup1-10cm from Target, FC2-5cm from Target)

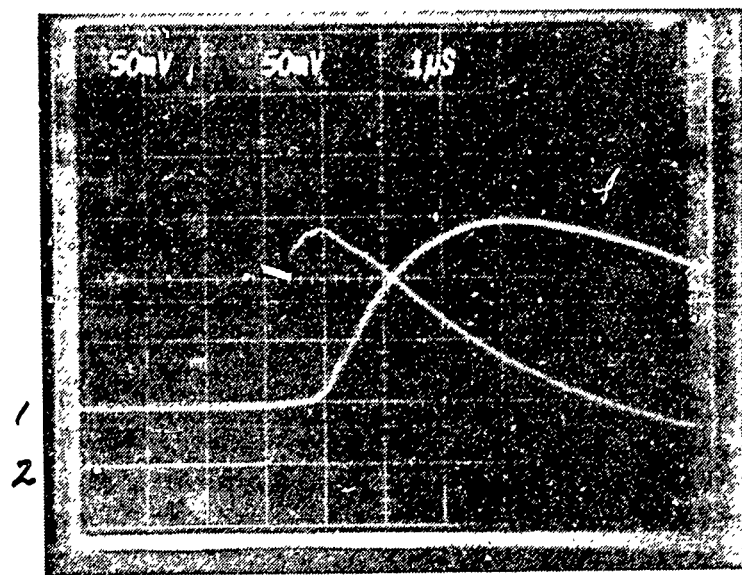


Figure 30. Distance Gap 10 cm, Probe Bias Voltage -20 V, in Parallel Orientation  
(FC1-15cm, FC2-5cm)

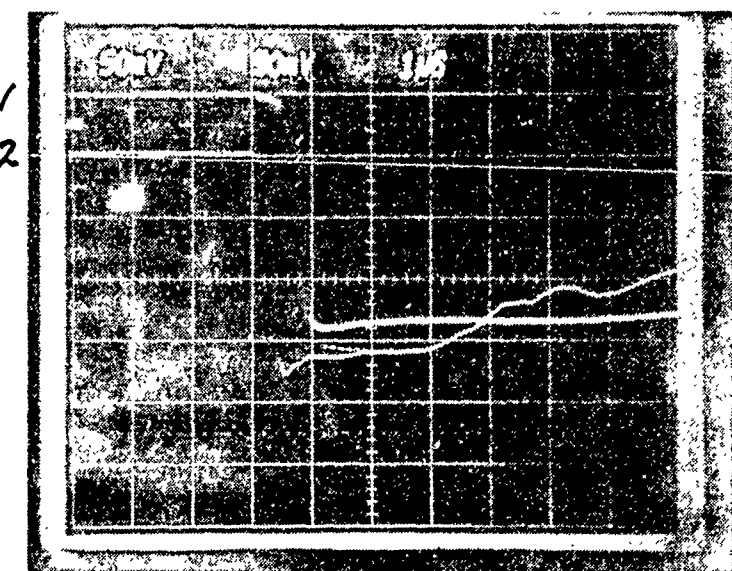


Figure 31. Distance Gap 5 cm, Probe Bias Voltage + 20 V, in Parallel Orientation  
(FC1-10cm, FC2-5cm)

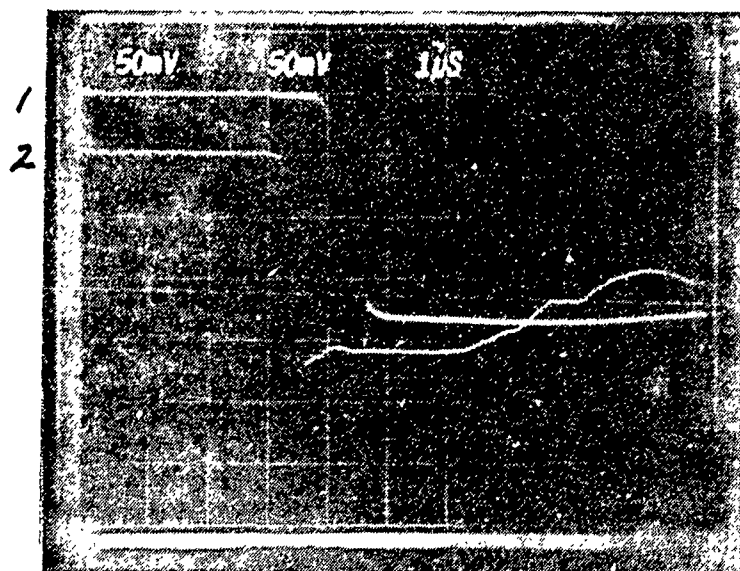


Figure 32. Distance Gap 10 cm, Probe Bias Voltage + 20 V, in Parallel Orientation  
(FC1-15cm, FC2-5cm)

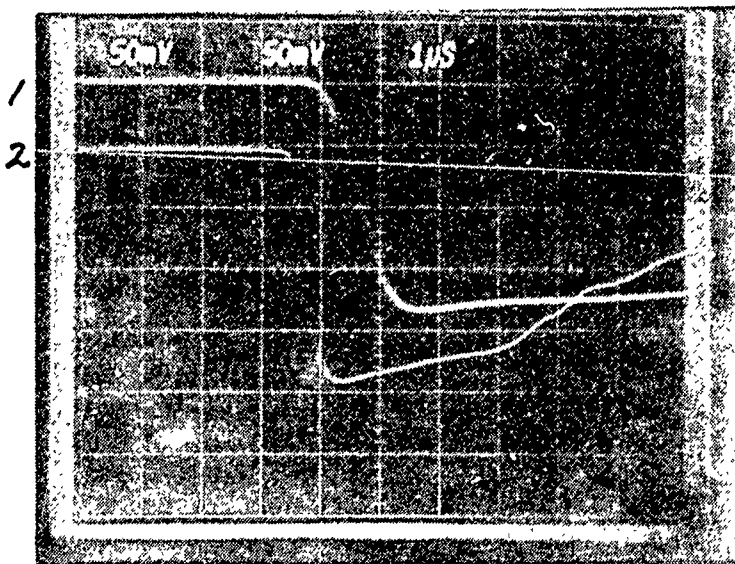


Figure 33. Distance Gap 5 cm, Probe Bias Voltage + 20 V, in Perpendicular Orientation (FC1-10cm, FC2-5cm)

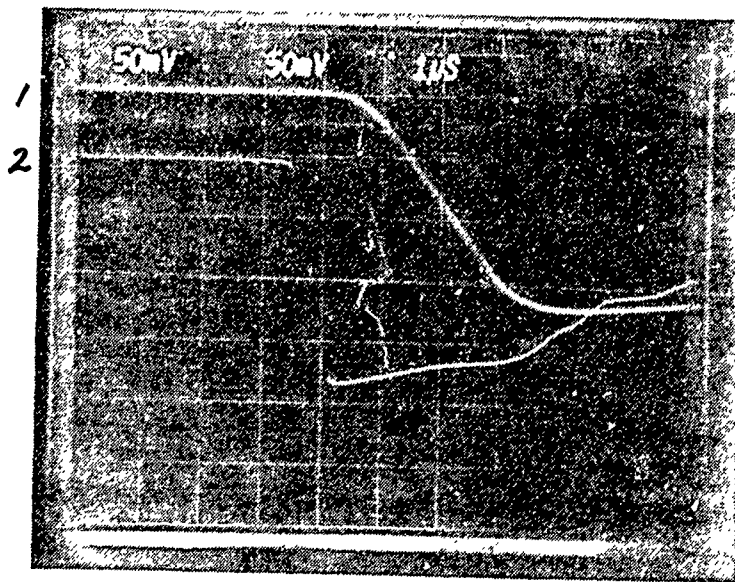


Figure 34. Distance Gap 10 cm, Probe Bias Voltage + 20 V, in Perpendicular Orientation (FC1-15cm, FC2-5cm)

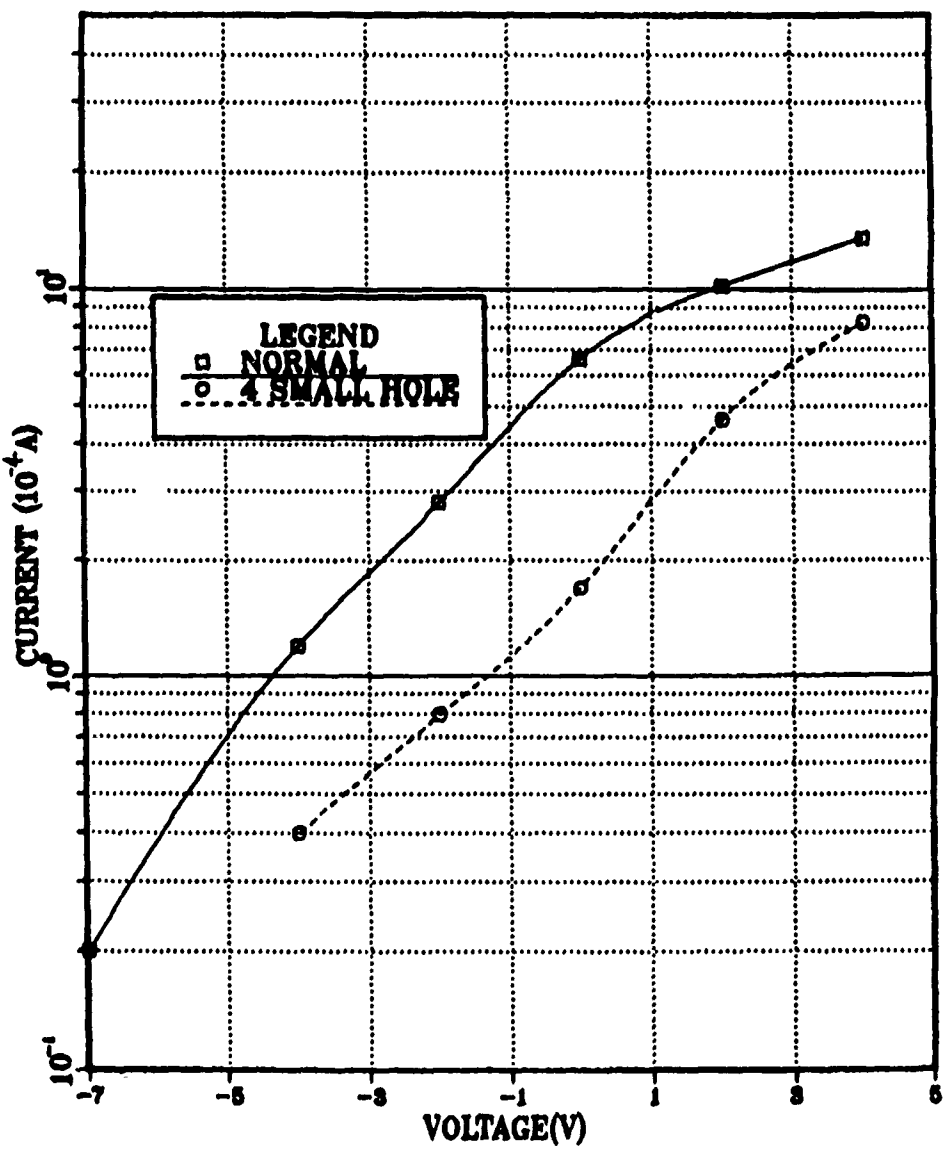


Figure 35.  $\ln I_e$  vs Probe Bias Voltage

### 3. Plasma Density

Several approaches were taken to derive the plasma density. In this series of experiments, Faraday cups were located 10 cm from the target with the Faraday cup orientation perpendicular to the direction of plasma flow. Current-voltage characteristic curves were obtained by recording current versus time for a series of Faraday cup voltages. Then, for a given time after the firing of the laser, curves of currents as a function of Faraday cup potentials were plotted.

The ion plasma density,  $n_i(cm^{-3})$ , is derived using the equation (2.23)

$$j_i = env_i \quad (2.23)$$

where  $j_i$  = ion saturation current density.

From the Bohm criterion for the formation of an ion sheath follows

$$v_{i\perp} = \sqrt{\frac{KT_e}{M_i}}.$$

Using  $T_e = 2.4$  eV from figure 35 and the proton mass (Lexan), then  $v_{i\perp} = 1.5 \times 10^4$  cm/sec, and the ion saturation current density was calculated from Tables 1, 2 and Figure 37. The ion saturation current density was  $j_i = 0.11 A/cm^2$  for the one hole Faraday cup, and  $j_i = 0.03 A/cm^2$  for the 4 small holes. Therefore,  $n_i = \frac{j_i}{ev_i} = 4.54 \times 10^{13}(cm^{-3})$  in the first case, and  $1.24 \times 10^{13}(cm^{-3})$  in the latter.

Using the Bohm approximate formula (4.2) for the ion saturation current

$$I_i \approx 0.4en \sqrt{2 \frac{KT_e}{M_i}} A \quad (4.2)$$

where, A = Faraday cup hole area

$$[\text{one hole} = 3.33 \times 10^{-3}(cm^2)]$$

$$[\text{4 small holes} = 3.91 \times 10^{-3}(cm^2)]$$

The measured ion saturation current from Figure 37, was  $I_{io} = 3.6 \times 10^{-4} (A)$ , and  $I_{io} = 1.0 \times 10^{-4} (A)$  for one and 4 holes respectively. Therefore,  $n_i \approx 7.88 \times 10^{13} cm^{-3}$  (one hole),  $n_i \approx 1.86 \times 10^{13} cm^{-3}$  (4 small holes).

Electron plasma density,  $n_e (cm^{-3})$  is derived from the electron saturation current using the equation (4.3)

$$I_{eo} = \frac{-1}{4} n_e \bar{v}_e A e \quad (4.3)$$

where,  $I_{eo}$  = electron saturation current

$$\bar{v}_e = \text{mean thermal velocity} = \sqrt{\left(8 \frac{KT_e}{\pi m_e}\right)} = 1.04 \times 10^6 cm/sec$$

$A$  = Faraday cup hole area.

The electron saturation current was estimated  $I_{eo} = -13.3 \times 10^{-3} A$  (one hole),  $I_{eo} = -11.3 \times 10^{-3} A$  (4 small holes) from Figure 39. Therefore, all the data put into equation (4.2), then calculated  $n_e = 9.6 \times 10^{13} cm^{-3}$  (one hole)  $n_e = 6.95 \times 10^{13} cm^{-3}$  (4 small holes).

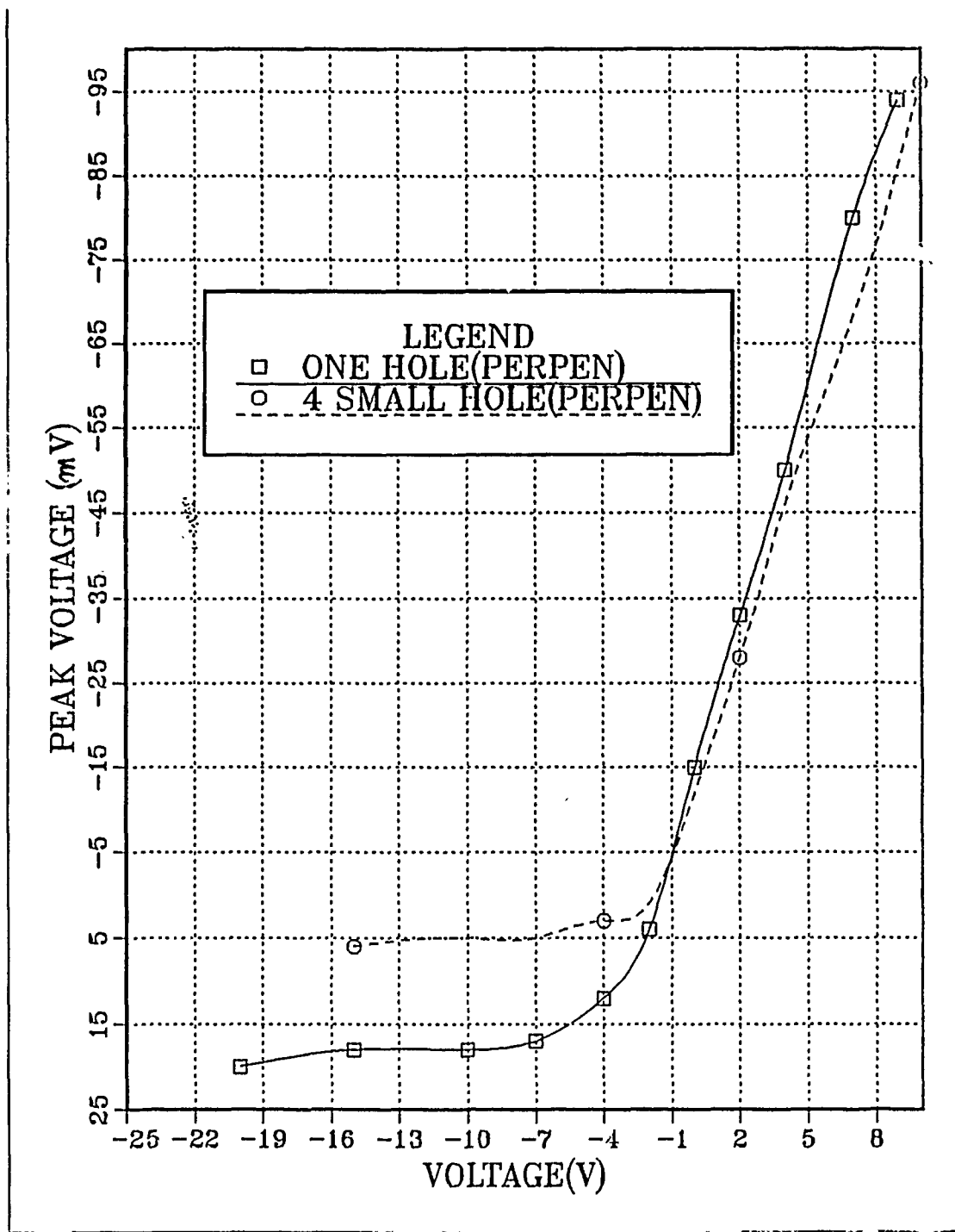


Figure 36. Peak Voltage vs Bias Voltage (-20 V to +10 V ), Distance d = 10cm

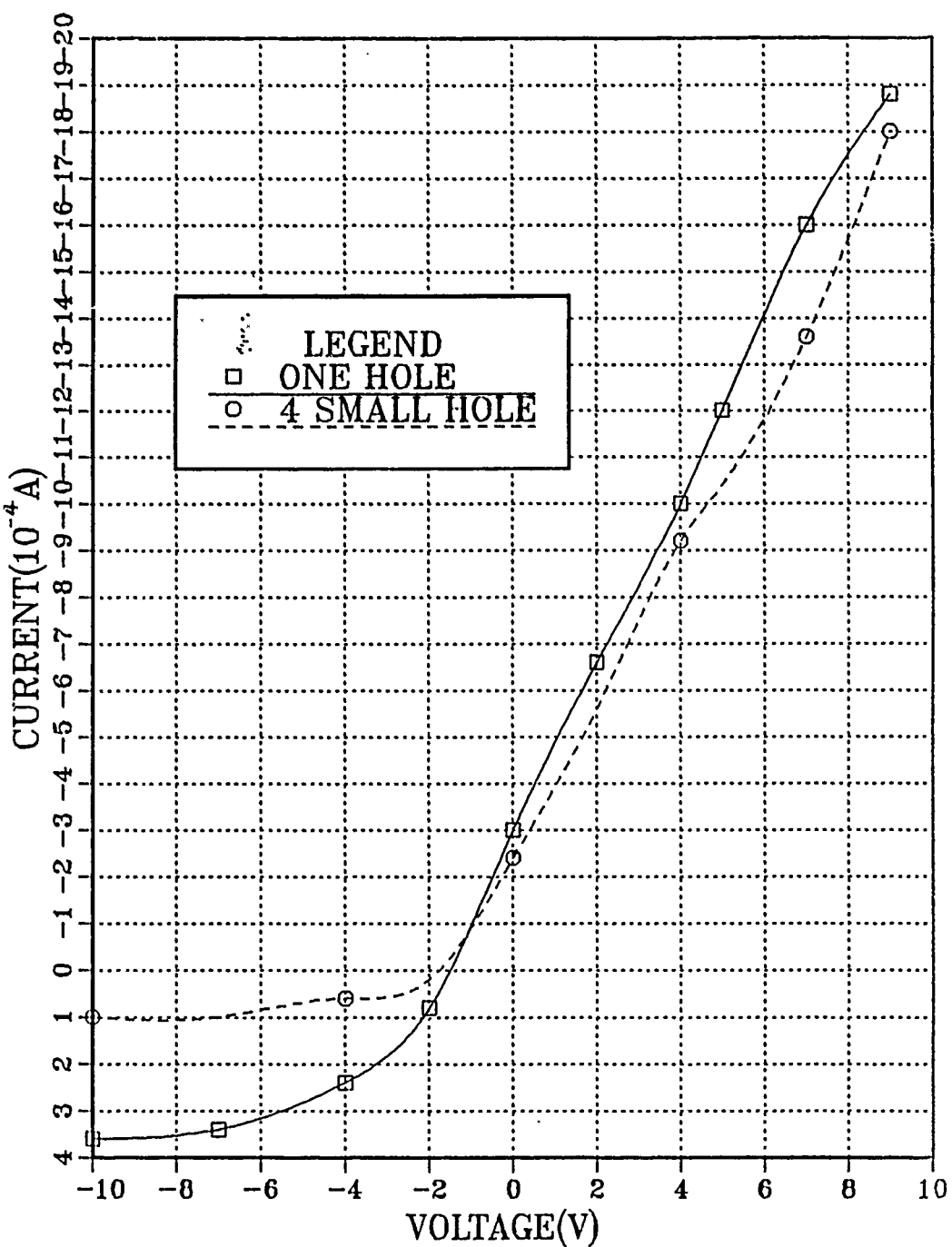


Figure 37. Current vs Bias Voltage (-10 V to +7 V ), Distance  $d = 10\text{cm}$

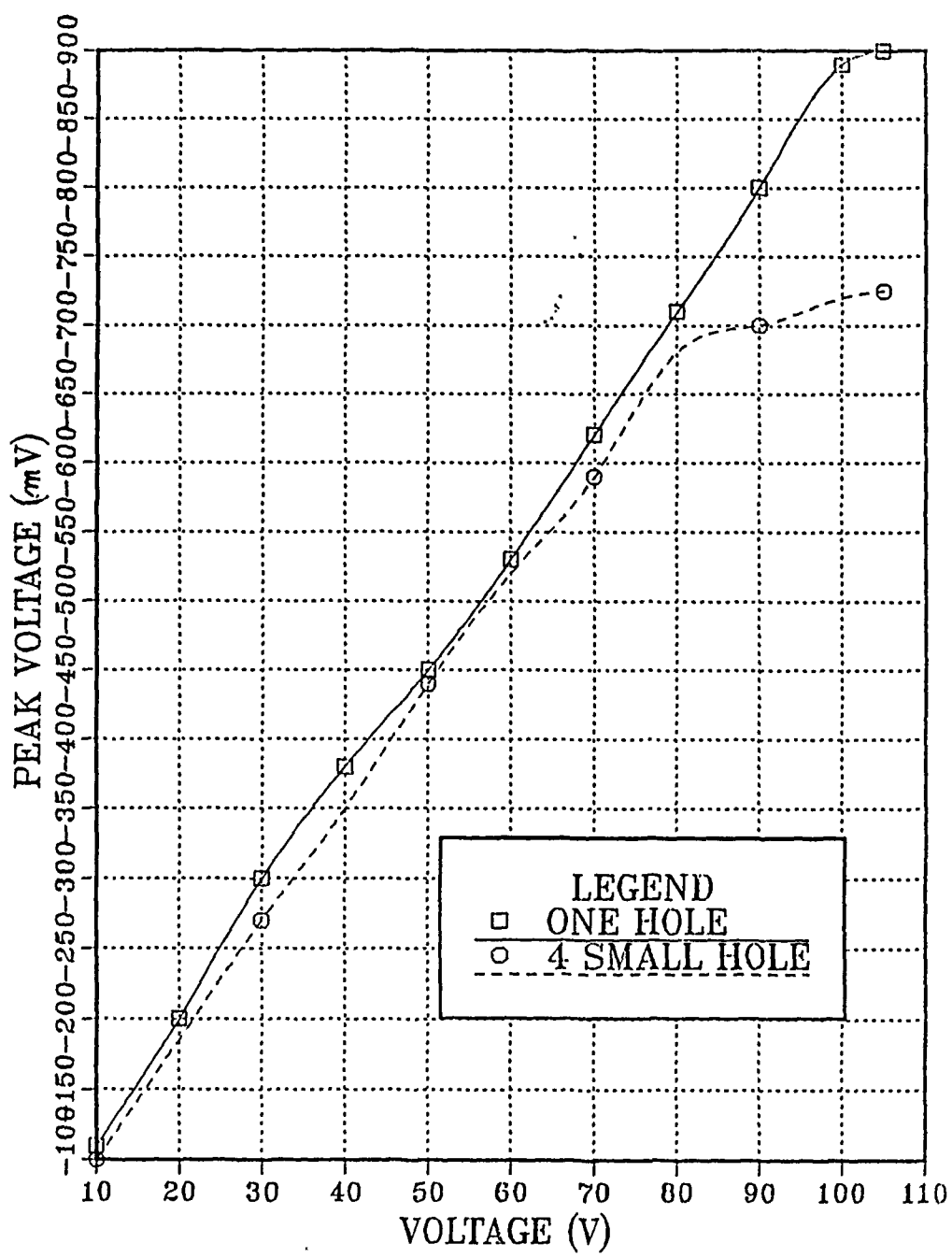


Figure 38. Peak Voltage vs Bias Voltage (0 v to + 105 V ), Distance d = 10cm

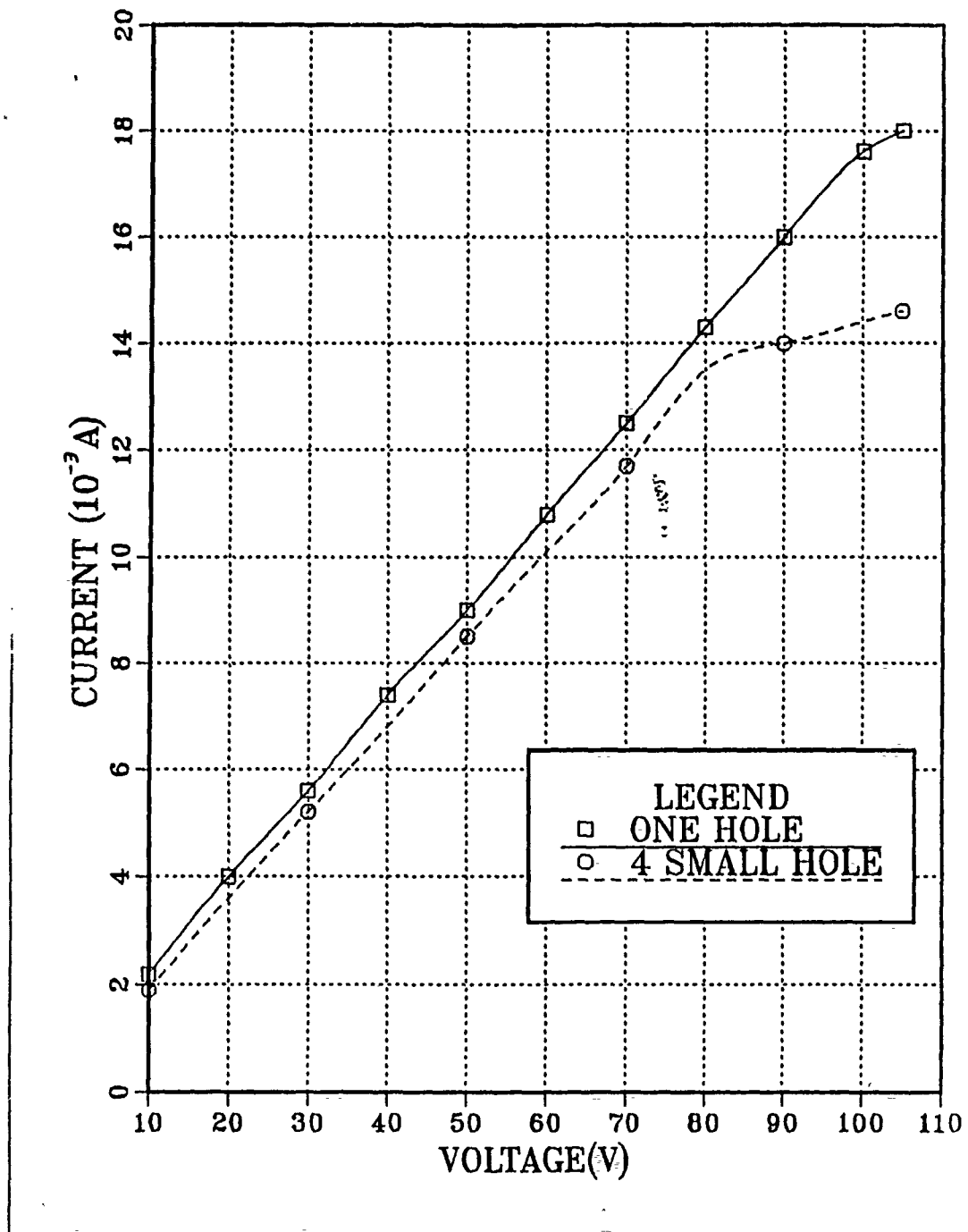


Figure 39. Current vs Bias Voltage (0 V to + 105 V ), Distance d = 10cm

Table 1. VOLTAGE, CURRENT, CURRENT DENSITY MEASURED WITH FARADAY CUP WITH ONE ENTRANCE HOLE ( D=10CM )

probe voltage(V)	peak voltage(mV)	current( $10^{-3}A$ )	current density ( $A/cm^2$ )
-20	20	0.4	0.12
-10	18	0.36	0.11
-7	17	0.34	0.1
-4	12	0.24	0.07
0	-15	0.3	0.09
10	-100	2	0.6
20	-200	4	1.2
30	-300	6	1.8
40	-380	7.6	2.28
50	-430	8.6	2.58
60	-550	11	3.3
70	-620	12.4	3.72
80	-720	14.4	4.32
90	-800	16	4.8
100	-890	17.8	5.35
105	-900	18	5.4

**Table 2. VOLTAGE, CURRENT, CURRENT DENSITY MEASURED WITH FARADAY CUP WITH 4 SMALL ENTRANCE HOLES( D = 10CM )**

probe voltage(V)	peak voltage(mV)	current( $10^{-3}A$ )	current density ( $A/cm^2$ )
-20	6	0.12	0.03
-10	5	0.1	0.025
-7	5	0.1	0.023
-4	3	0.06	0.015
0	-12	0.24	0.06
10	-96	1.92	0.49
20	-185	3.7	0.9
30	-250	5	1.28
40	-340	6.8	1.74
50	-440	8.8	2.25
60	-520	10.4	2.66
70	-590	11.8	3.02
80	-680	13.6	3.48
90	-700	14	3.58
100	-720	14.4	3.68
105	-760	15.2	3.89

## V. SUMMARY AND DISCUSSION OF RESULTS

The objective of this experiment was to perform measurements on laser produced plasma using Faraday cups. Current signals were measured at different distance from the target and at variable probe bias voltage.

### A. SUMMARY OF RESULTS

In order to support the analysis of the data to be presented, a summary of the results follows :

1. The shielding distance can be computed from the Debye length with the electrostatic potential replacing the usual thermal energy.
2. The use of the Faraday cup detectors with electrostatic separation of ion and electron component of an expanding laser produced plasma offers some insight into the dynamics of the plasma expansion.
3. The plasma expansion velocities measured was determined to be  $1.25 \times 10^7$  cm/sec.
4. The electron temperature was evaluated from the semi-logarithmic plot of the electron repelling part of the characteristics. It was found from Figure 35, that  $T_e = 2.4 eV$ , 10 cm from the target surface.
5. Electron saturation current was almost  $10^{-3}(A)$ , ion saturation current was nearly  $10^{-4}(A)$ , as shown Figures 37 and 39.
6. The plasma ion and electron density was approximately  $10^{13} cm^{-3}$  at the distance of 10 cm. since the plasma was quasineutral the density of ions,  $n_i$  and the density of electrons,  $n_e$ , might be approximately equal. therefore, the plasma density is

$$n_i \approx n_e \approx n .$$

### B. DISCUSSION OF RESULTS

The plasma potential may not be defined experimentally by a clear change in the behavior of the current characteristic, and that the current to the probe at plasma potential will be greater than the thermal current to the probe in the sta-

tionary plasma case [Ref. 17]. The ion current is given by the ion flux intersecting the area of the Faraday cup projected normal to the direction of flow, an approximation which should be very good for the energetic ions found in a laser produced plasma.

The sparking potential  $V$  against  $Pd$  correlate for the following reasons: ( where,  $P$  = pressure,  $d$  = distance between cover and detector ) The number of molecules in the gap is proportional to  $(Pd)$ . At low  $P$ ,  $\lambda$  ( mean free path ) is large and few electrons can collide with gas molecules ; most of them impinge on the cup and few ionizations take place. In order to have a number large enough for breakdown to occur,  $V$  has to be larger as  $P$  becomes smaller. At large  $P$ , however,  $\lambda$  is small and few electrons acquire sufficient energy over a mean free path to ionize. Hence most of the electrons produce electronic or molecular excitation. In order to produce enough ionization in the gap,  $V$  must be large and is higher for larger  $P$ . A similiar argument would apply for a variation of  $d$ . In this experiment, sharp and thick rim of Faraday cup detector shows larger peak voltage than detector with thin and round rim (i.e. larger amplitude ).

Current-Voltage characteristic curves were obtained by recording current versus time for a series of probe voltages ; then, for given times after the firing of the laser, currents were plotted as a function of probe potentials.

The saturation of ion current for negative voltages is clearly evident. The floating potential, for which  $I = 0$ , occurs at  $V \approx 0$ , as described in the previous chapter of this thesis.

In the vicinity of the floating potential, the current appears to increase exponentially with voltage relative to the saturation ion current. At a potential of a few volts negative relative to ground, the characteristic curve changes its curvature and appears to level off to the ion saturation current. At positive potentials, however, the current increases approximately linearly with voltage.

In the parallel orientation the Faraday cup characteristic corresponds to double probe, if the hole diameter was greater than the Debye length. Under this condition equal electron and ion current would flow into the Faraday cup.

## VI. CONCLUSION AND RECOMMENDATIONS

In this investigation the focused beam of single pulses from a  $CO_2$  laser was used to irradiate Lexan targets within a vacuum chamber. The Faraday cup was placed inside the vacuum chamber, and signals received were displayed on an oscilloscope. Targets were irradiated at a pressure of  $10^{-5}$  Torr.

The objective of this experiment was to evaluate laser produced plasma using Faraday cups. The flow velocity, the density and the electron temperature of the plasma were determined. The use of the Faraday cup detectors with electrostatic separation of ion and electron components of an expanding laser produced plasma offers some insight into the dynamics of the plasma expansion.

Faraday cups transverse to high velocity plasma flows, may be used as diagnostic tools in expanding laser plasmas and similiar environments.

In order to pursue the results of this research, the following recommendations for future research are presented :

1. Investigate the plasma velocities of laser-target interaction using Faraday cup, but with different target materials (metals). An increase in plasma ion mass should markedly reduce their velocities.
2. A concurrent project for further research is to use alternate plasma diagnostic techniques for examination of the laser produced plasma characteristics.
3. An investigation of plasma expansion velocity and plasma density should be conducted for varing background pressure and irradiances.

It is hoped that this study will help to stimulate further interest and research into the measurement on the laser produced plasma using Faraday cups.

## **APPENDIX A. LUMONIC TE-822 HP CO<sub>2</sub> LASER OPERATING PROCEDURE**

The CO<sub>2</sub> high energy pulsed laser is the primary research instrument for the study of plasma surface interactions at the Naval Postgraduate School. It must be operated in strict accordance with the operating procedures and safety precautions as established by prior research and updated in this appendix [ A, B ].

Prior to operating the laser system, an individual should complete a retina scan eye examination, receive an orientation briefing from the Physics Department's Lab technician, and become thoroughly familiar with all procedural and safety aspects of the laser system.

During the orientation briefing, the potential hazards and safety requirements associated with the laser system should be stressed. The most detrimental hazard is the invisible CO<sub>2</sub> beam (10.6 microns) which is outside the visible range. Inadvertent exposure of the eyes and other body parts could result in injury; therefore, eye protection should be worn by all personnel, the target container confinement facility should be completely closed, and all interlocks should be operational before the laser is fired. UNDER NO CIRCUMSTANCE should an interlock be overridden unless the Physics Department's Lab technician is present or notified. The electrical interlocks, which are contained in the laser pulse initiation circuit, include :

### **1. Laser Enclosure Cover Interlocks (2)**

Ensure that the laser cabinet covers are in place to prevent electrical shock from the high voltage power supplies and other interior electrical components.

### **2. Laser Output Port Protective Cover Interlock**

Ensures that the laser is not inadvertently pulsed with the output port protective cover in place causing reflection back into the internal optics of the laser.

### **3. Cooling Water Flow**

Ensures that proper cooling water flow and pressure are maintained in the laser system so that the temperature sensitive high voltage power supplies do not overheat and fail on thermal overload. Thermal interlocks associated with the high voltage power supplies are designed to trip on temperatures in excess of 125 degrees Fahrenheit.

### **4. Laser Power Key**

Ensures that power is not available to the laser system until consciously applied by the operator.

### **5. Gas on / off Switch**

Ensures that high voltage is not applied to the firing circuit unless gas flow has been properly established in the laser.

### **6. Plasma Laboratory Door**

Ensures that the laser firing circuit will be temporarily disabled if the laboratory door is opened during laser system operation. An audible alarm alerts operators of this problem.

Although the interlock system does afford considerable safety, electrical interlocks can never replace the requirement for an alert and conscientious operator. It is with this in mind that the following operational procedure contained within the Lumonics TE-822 HP instruction manual [Ref.10].

## **A. LASER SYSTEM START-UP**

1. Turn on the external voltage regulator and adjust its output for 119 volts.

### **NOTE**

The high voltage power supplies inside the laser are NOT regulated ; therefore, it is necessary to regulate the input voltage in order to acquire consistent laser output and performance characteristics.

2. Activate the laboratory door interlock by placing the toggle switch on the control box to the left of the door to the on position.

3. Initiate cooling water flow and set the thermostat on the cooling unit to 15 degrees celsius.

4. Set the mode select switch to single and the MULTIPLIER setting to X10.

#### NOTE

The MULTIPLIER control setting has three positions which are X1, X10, and X100. Three setting are used in conjunction with the INTERNAL RATE potentiometer and apply their stated multiplication factors to establish a desire pulse repetition frequency. IN the X1 and X10 positions the capacitors in the laser firing circuit are continuously charged, and the front panel voltmeter continuously registers the high voltage power supply voltage level. IN SINGLE shot mode, repetitive pulsing is not possible but the X10 MULTIPLIER setting is used so that the high voltage power supply voltage can be monitored continuously during the conduct of the laser start up procedure.

#### 5. Open the Helium, Carbon Dioxide and Nitrogen Cylinder valves.

#### NOTE

The pressure regulators on each bottle are not adjustable until the gas is flowing through the laser system.

#### 6. Turn the LASER POWER KEY to ON and note that the GAS OFF indicator is GREEN, the INTERLOCKS OPEN indicator is WHITE and the WARM UP INCOMPLETE indicator is YELLOW.

#### NOTE

The WARM UP INCOMPLETE indicator will extinguish after approximately 1 minute after the LASER POWER KEY is turned on.

#### 7. Slowly open the HEAD EXHAUST VALVE by placing the valve operator in the vertical position. The valve is located in the lower right hand corner of the control panel.

#### CAUTION

Failure to open the HEAD EXHAUST VALVE can cause the head to quickly become overpressurized. The laser is equipped with a NON-RESETTABLE 5 psig pressure relief valve which requires maintenance personnel to replace. Failure to open this relief valve will place the laser system out of commission until a replacement valve is installed. If there is excessive use of gas or if the laser energy is extremely erratic, notify the Physics Department

Lab Technician, open the laser cabinet, and check for gas leaks ; these are the signs of a blown head gasket.

8. Depress the GAS ON push button and observe the RED GAS ON indicator is lit while the GREEN GAS OFF indicator is extinguished.

9. After 15 seconds, adjust the pressure regulators to 10 psig.

10. Adjust the six Brooks flowmeters (three on the front control panel and three on the rear panel ) to the following reading : 8 SCFH for  $N_2$  and  $CO_2$  , and 6 SCFH for He.

#### NOTE

The gas flow rates have been established for plasma research at the Naval Postgraduate School. These flow rates will produce single shot energies up to 15 joules with pulse widths of approximately 5 microseconds. These flow rates can be changed in accordance with the Lumonics laser instruction manual.

#### NOTE

Continually monitor the pressure regulators and Brooks flowmeters throughout the operation of the laser to insure that the pulse width and energy output of the laser do not change. Fluctuation in the gas flow rate can change the pulse width and laser output significantly.

11. Remove the LASER OUTPUT PORT PROTECTIVE COVER.

#### CAUTION

Failure to remove the LASER OUTPUT PORT PROTECTIVE COVER could result in damage to the internal optics of the laser. There is an electrical interlock to prevent the firing of the laser with the cover in place ; however, it should be physically verified that the cover or alignment mirror has been removed before firing.

12. Allow the gas to flow through the laser cabinet for 30 minutes before firing the laser.

#### NOTE

Do not stop the gas flow once it has been initiated except when a delay of more than 30 minutes will occur. The  $CO_2$  Will diffuse out of the molecular sieve inside the laser cavity thereby producing erratic shots.

13. Open the air cylinder and set the pressure regulator to 18 psig and establish a flow rate of 4 SCFH by adjusting the 6 flowmeters on the rear panel.

14. After the 30 minute warm up time is complete, prepare for an alignment checks of the laser.

**NOTE**

Before every firing period, it is strongly recommended that the burn pattern and laser alignment are verified. Temperature changes, removal of laser cabinet covers, and earth quakes can shift the alignment of the laser.

15. Put a piece of black weighing paper on a brick, and place the brick at the alignment verification spot located inside the target containment area. Insure that the laser beam path is clear of all obstacles except the bricks.

**CAUTION**

The target containment facility should have the door and windows closed at this point. **NO ONE SHOULD BE INSIDE THE TARGET CONTAINMENT FACILITY.** All personnel should always put eye protection on anytime the high voltage power supply is going to be activated.

16. Set the HV CONTROL KNOB fully counterclockwise to its MINIMUM setting and depress the RED HIGH VOLTAGE ON push button.

17. Turn the HV CONTROL KNOB clockwise until the voltmeter indicates 25 HV.

**CAUTION**

NEVER allow the high voltage to exceed 40 HV. the laser can operate at 40 HV at a slow single pulse rate of one shot every minute ; however, the laser designer recommends using the laser at settings of 36 HV and below to avoid damage to the high voltage power supplies and internal optics.

18. The laser will now fire each time the SINGLE fire push button is depressed. Check to insure the chamber is clear and all personnel are wearing eye protection, and press the SINGLE fire push button.

19. Press the GREEN HIGH VLOTAGE OFF push button.

**CAUTION**

The GREEN HIGH VOLTAGE OFF push button should be illuminated before entering the target containment area to prevent accidental of the laser.

**NOTE**

The burn pattern for this laser is approximately a rectangle with dimensions 30 mm by 33 mm. If the burn pattern is not uniform, a cavity realignment will be necessary as described by the Lumonics laser instruction manual. If the HV setting is 21 or below, the burn pattern will be nonuniform.

20. Place the alignment mirror on the laser output port, turn on the He Ne laser, and verify that the center of the damaged area on the wieghing paper does in fact correspond to the alignment spot in the target containment facility. If the alignment is correct, the laser is prepared for research. If the alignment spot does not correspond to the center of the damaged area, either realign the laser as described in the Laser Instruction Manual or mark a new spot if the alignmnet is close.

21. While using the He Ne laser to align the optical components of the system, align the beam splitter and the energy meter probe. Place a brick in the reflection line of site as a dump for the  $CO_2$  laser.

**WARNING**

All optics and detector surfaces should be free of dust. Use canned gas to remove the dust.

22. Remove the alignment mirror, close the target cotainment facility, and put on eye protection. Push the RED HIGH VOLTAGE ON push button, push the SINGLE fire push button, and observe the energy meter reading.

23. Adjust the HV CONTROL KNOB setting on the front panel to the desire energy otuput.

**NOTE**

Verify the energy output of the lascr before irradiating targets if more than 5 minutes has elapsed since the previous firing. This verification will reduce the amount of fluctuation inevitable with a  $CO_2$  laser.

## **B. LASER SYSTEM SHUT DOWN PROCEDURES :**

1. Insure that the GREEN HIGH VOLTAGE OFF push button is illuminated
2. Close all of the gas tanks
3. Wait until all SCFH meters are reading zero, and then push the GAS OFF push button.
4. Close the HEAD EXHAUST VALVE.
5. Turn the LASER POWER KEY to OFF

### **WARNING**

Before turing off the cooling unit, the HEAT light must be illuminated. If necessary increase the temperature of the cooling unit the HEAT light illuminates.

6. Turn off the cooling unit.
7. Cover the LASER OUTPUT PORT.
8. Turn off the door interlock switch and the audible alarm switch.
9. Cover the laser with the electric blanket and turn the blanket on the setting of 6.

### **NOTE**

It is only necessary to turn on the electric blanket to maintain the optics of the laser at a constant temperature. If the laser is not going to be in use for several days, then temperature control of the optics is not required.

10. If the laser is not going to be utilized for several days, turn off the external voltage regulator.

## APPENDIX B. VEECO 400 VACUUM SYSTEM OPERATING PROCEDURES

The VEECO 400 Vacuum System is utilized in conjunction with the  $CO_2$  laser for research of plasma surface interactions. Targets can be irradiated with the  $CO_2$  laser in reduced pressure conditions ranging from 760 torr to  $10^{-6}$  Torr. This system must be operated in strict accordance with the updated operating procedures as established in this appendix [ Ref. 11 ].

Prior to operating the vacuum system, an individual should receive an orientation briefing from the Physics Department's Lab technician and become thoroughly familiar with all procedure and safety aspects of the vacuum system.

During the orientation briefing, the potential hazards and safety requirements associated with the vacuum system should be stressed. The most significant of these hazards are the exhaust fumes that can develop if the exhaust system fails and the electrical danger created if the cooling hose breaks. Upon detection of any unusual odors, leaks or sounds, the Physics Department's Lab technician should be immediately notified. It is with this in mind that the following operational procedure is provided.

### A. VACUUM SYSTEM START-UP

Figure depicts the position of the controls on the VEECO vacuum system referenced in the following instructions in Figure 40 on page 72.

#### NOTE

CLOCKWISE rotation of the vents or valves CLOSES them. COUNTER-CLOCKWISE rotation opens the valves.

#### WARNING

When ever any valve is opened, rotate the control counter-clockwise SLOWLY to avoid damaging the vacuum system.

1. Close all valves and vents.
2. Set the pressure MULTIPLIER KNOB to  $10^{-4}$  position.

3. Turn on the MECHANICAL PUMP ON/OFF SWITCH. Let the mechanical pump run for approximately 30 minutes to outgas the oil reservoir.

NOTE

The time to outgas the oil reservoir depend on how long the pump has been off.

4. Open the FORELINE VALVE to allow the diffusion pump oil to be outgassed.

5. Turn on the vacuum gauge using the POWER ON/OFF SWITCH. The POWER ON BLUB should illuminate.

6. Set the TC-1/TC-2 THERMOCOUPLE SWITCH to the TC-1 position.

NOTE

TC-1 allows observation of the pressure in the foreline subsystem of the vacuum system. TC-2 allows observation of the pressure of the chamber.

7. Turn on the cooling tap water.

WARNING

if the diffusion pump on/off switch is turned without the flow of the cooling water, the diffusion oil overheats and evaporates causing the heating coil to burn out.

8. When the thermocouple gauge gets below 20 microns, turn on the diffusion pump on/off switch.

NOTE

As the diffusion oil heats, the pressure on the thermocouple gauge will increase initially, and then begin decreasing again. The diffusion pump is wired to a flow switch on the cooling water line. The flow switch will turn off the diffusion pump if there is a loss of cooling water flow.

9. Add liquid nitrogen to the cold trap.

10. After 20 minutes, turn on the ion gauge by pressing the FILAMENT CURRENT ON push button. The FILAMENT ON BLUB should illuminate.

## B. HIGH VACUUM CHAMBER OPERATION

1. Close the FORELINE VALVE.
2. Switch the TC-1/TC-2 THERMOCOUPLE SWITCH to the TC-2 position.
3. Open the ROUGHING VALVE.

### WARNING

In the following step, be sure that the IONIZATION GAUGE does not go off scale.

4. When the THERMOCOUPLE GAUGE reads below 50 microns, CLOSE the ROUGHING VALVE, and OPEN the FORELINE VALVE. SLOWLY open the HIGH VACUUM VALVE.

5. When the IONIZATION GAUGE gets below  $0.2 \times 10^{-4}$  torr, switch the PRESSURE MULTIPLIER KNOB to  $10^{-5}$  Torr.

6. After the pressure gets below  $5 \times 10^{-5}$  Torr, Switch up the READ CURRENT SWITCH to read the emission current. it should read 10 ma ; if not, adjust it using the CURRENT ADJUST KNOB and CURRENT SET KNOB.

### NOTE

It will probably be necessary to outgas the ion for approximately 15 minutes in order to read higher vacuum.

7. Turn on the DEGAS ON /OFF SWITCH. The filament may trip, and the FILAMENT ON BLUB may extinguish. Wait 1 minute and push the FILAMENT CURRENT ON push button again. If the filament bulb extinguishes again, wait five minutes and try again.

8. When the IONIZATION GAUGE reaches  $0.2 \times 10^{-5}$  torr, switch the PRESSURE MULTIPLIER KNOB to  $10^{-6}$  Torr.

## C. OPENING THE CHAMBER

1. Set the PRESSURE MULTIPLIER KNOB to  $10^{-4}$  setting.
2. Close the HIGH VACCUM VALVE.
3. Slowly open the CHAMBER VENT. After the air has stopped flowing into the chamber, it can be opened.

#### **D. SYSTEM IDLING CONDITION**

1. Complete the HIGH VACCUM CHAMBER OPERATION to evacuated the chamber.
2. Close the HIGH VACCUM VALVE.
3. Press the FILAMENT CURRENT OFF push button.

##### **NOTE**

The vacuum system can operate in this configuration for several days until the next experiment is conducted.

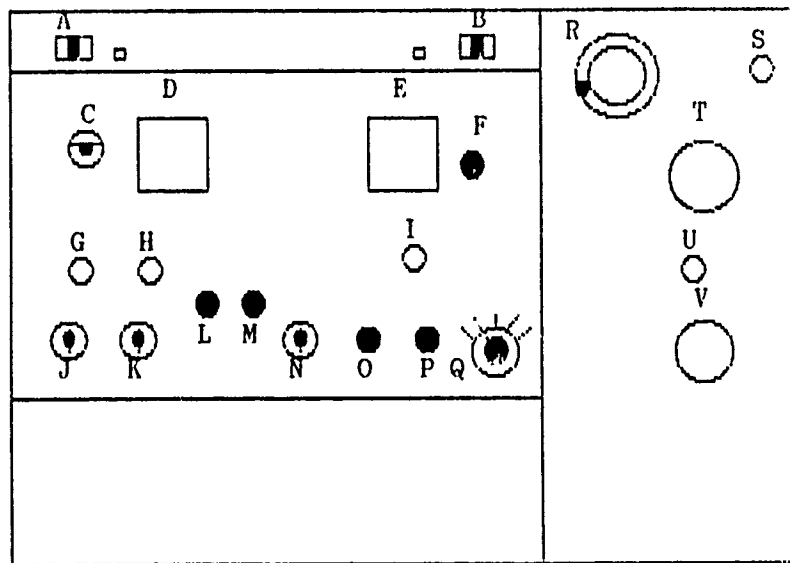
#### **E. SHUT DOWN THE SYSTEM COMPLETELY**

1. Press the FILAMENT CURRENT OFF push button.
2. Close the HIGH VACCUM VALVE and the ROUGHING VALVE.
3. Turn off the DIFFUSION PUMP SWITCH.

##### **WARNING**

Let the diffusion pump cool down for at least 30 minutes to avoid damping the pump before pressing with these procedures.

4. Close the FORELINE VALVE.
5. Turn off the cooling water.
6. The mechanical pump can be left running in this position indefinitely. To secure the mechanical pump, turn off the MECHANICAL PUMP ON / OFF SWITCH and open the MECHANICAL PUMP VENT for approximately 5 minutes. When the air flow has stopped, close the MECHANICAL PUMP VENT.



- A - MECHANICAL PUMP ON/OFF SWITCH
- B - DIFFUSION PUMP ON/OFF SWITCH
- C - TC-1/TC-2 THERMOCOUPLE SWITCH
- D - THERMOCOUPLE GAUGE
- E - IONIZATION GAUGE
- F - ZERO ADJUSTMENT
- G - POWER ON BULB
- H - DEGAS ON BULB
- I - FILAMENT ON BULB
- J - POWER ON/OFF SWITCH
- K - DEGAS ON/OFF SWITCH
- L - CURRENT SET KNOB
- M - CURRENT ADJUST KNOB
- N - READ CURRENT SWITCH
- O - FILAMENT CURRENT OFF PUSH BUTTON
- P - FILAMENT CURRENT ON PUSH BUTTON
- Q - PRESSURE MULTIPLIER VALVE
- R - HIGH VACUUM VALVE
- S - CHAMBER VENT
- T - ROUGHING VALVE
- U - MECHANICAL PUMP VENT
- V - FORELINE VALVE

Figure 40. VEECO Vacuum Chamber Controls

## APPENDIX C. SINGLE LANGMUIR PROBES

One of the most venerable of plasma diagnostic techniques involves the current-voltage characteristics of probes immersed in the plasma. Typical characteristics for a single probe, whose dimensions are small compared to electron and ion-free paths, are shown for a plasma, in the absence of magnetic field, in Figure 41 on page 74.

The probe potential is measured with respect to some convenient, fixed-potential point, such as the anode or walls of a discharge tube or a "floating probe". The requirement that the potential difference between the plasma and the reference point remain fixed often excludes the use of the anode for this purpose. The probe potential can be specified in respect to the plasma potential denoted by  $V$  (potential).

When  $V$  is made very negative all electrons are repelled and only ions are collected. The random ion current passing through an area  $A$  in the plasma is related to the ion density and the velocity :

$$I_i = \frac{J_i}{A_p} = n_i \frac{\bar{v}}{4} = \frac{n_i}{4} \sqrt{\frac{2KT}{m_i}} \quad (1)$$

where,  $I_i$  = the random ion current, Amp

$J_i$  = the random ion current density,  $Amp/cm^2$

$A_p$  = the area of the probe,

$m_i$  = the ion mass

$n_i$  = the ion density,

$\bar{v} = \sqrt{\frac{2KT}{m_i}}$  = mean kinetic ion velocity.

Equation 1 would be valid also for ion current collected by a probe if the presence of the probe caused no perturbation in the surrounding random plasma currents. The probe does perturb the plasma, however, the volume which the probe occupies provides an energy sink for all particles which strike it and the fringing fields

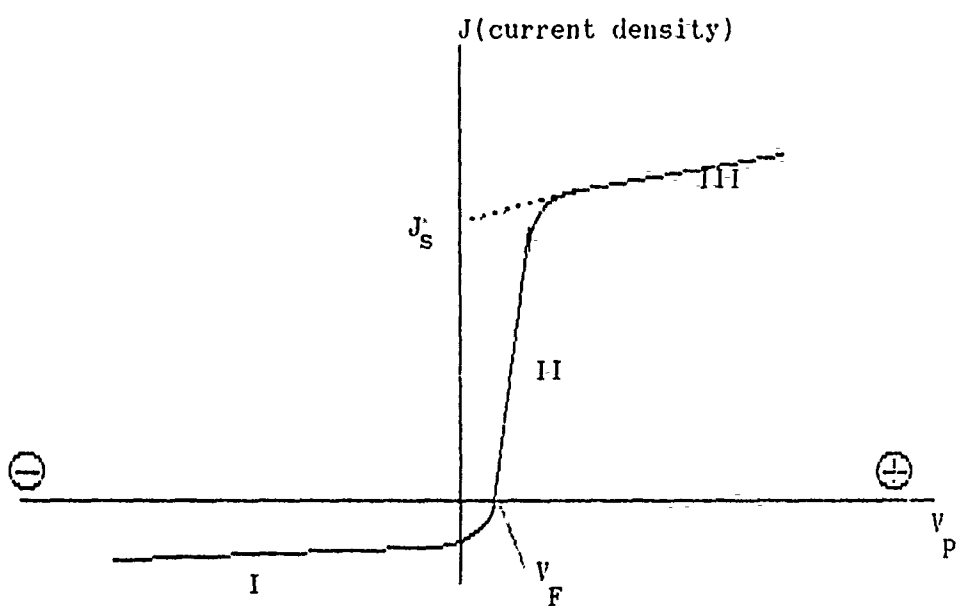
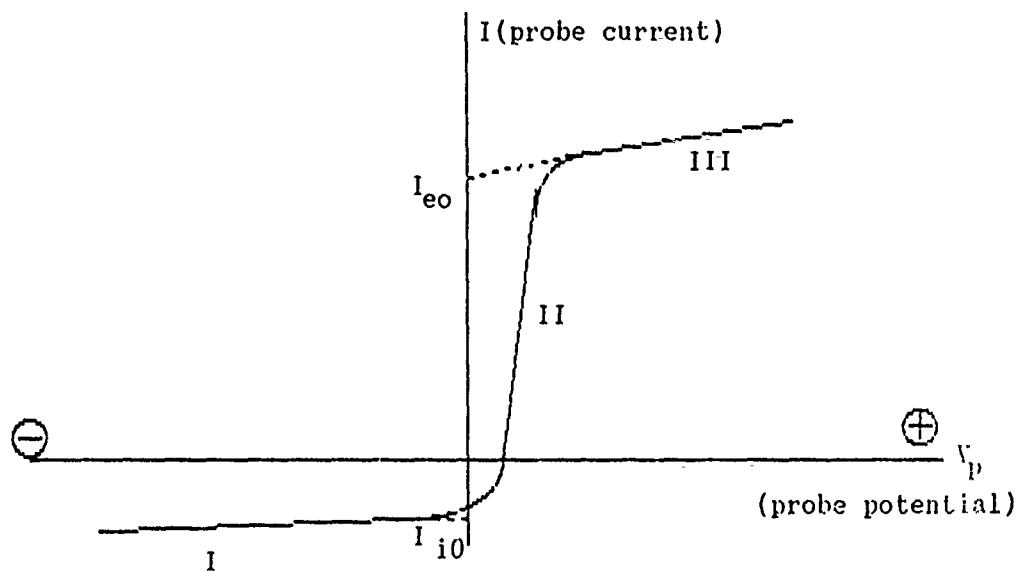


Figure 41. V-I Characteristics of Single Langmuir Probe

extend for a considerable distance into the surroundings. As a result, the collected ion current density seems to be more a function of the electron temperature than of the ion temperature. This effect is due to the formation of a positive sheath around the probe, caused by electrons repelled by the probe's electric field. The extent of the sheath's influence is determined by the electron temperature. For  $T_i < T_e$  the ion current density is nearly independent of the ion temperature, and equation 1 can be modified to :

$$J_i \approx 0.4 n_i \sqrt{\frac{2 K T_e}{m_i}} \text{ (Amp/cm}^2\text{)} \quad (2)$$

When the probe potential,  $V$ , is made less negative a few of the high energy electrons are collected, partially cancelling the positive ion current. As the potential is changed further in the positive direction the random ion and electron currents collected just cancel. This probe-plasma potential,  $V_f$  in Figure 41 is the "floating potential", the value at which a floating probe would ride when placed into the plasma.

Increasing  $V$  beyond  $V_f$  results in a steep rise in electron current, in region II (Figure 41). This current eventually saturates at the "space potential" value,  $V_s$ , due to space-charge limitation in current collection. According to our definition of  $V$ , we have  $V_s = 0$ . In region II the probe electron current follows a logarithmic dependence :

$$\ln I_e = \left( \frac{e}{K T_e} \right) V + \ln A J_0 \quad (3)$$

where ,  $A$  = the area of the probe sheath  $\approx A_p$

$J_0$  = the random electron current density ;

$J_0 = J_s + |J_i|$

$e$  = the electron charge.

The total probe current is the difference between the electron current and ion current, since it is the probe current,  $I$ , that we measure, to find  $I_e$  in equation 3 we write :

$$I_e = I + |I_i| \quad (4)$$

and

$$J_e = J + |J_i|$$

Equation 4 implies that the probe sheath is thin compared to probe dimensions, so that  $A_s \approx A_p$  is constant in size. This is not strictly true, since the sheath thickness is a function of the potential applied.

When we plot the logarithm of  $I_e$  vs probe voltage  $V$ , we obtain the slope of this curve in the region  $V \approx 0$ . If the electrons have a Maxwellian distribution the slope is constant and yields  $T_e$ :

$$\frac{d \ln I_e}{dV} = \frac{d \ln I_e}{dV_p} = \frac{e}{KT_e} \quad (5)$$

Increasing the probe voltage beyond  $V_s$  does not cause  $J$  to rise much higher than  $J_s$ , due to space charge. The saturation current is :

$$I_s = J_s A_s \approx J_0 A_s = \frac{en_e A_s}{4} \sqrt{\frac{2KT_e}{m_e}} \quad (6)$$

Comparing equation (6) with equation (2) we note that

$$\frac{J_s}{J_i} \approx \sqrt{\frac{m_i}{2m_e}}$$

The electron density can be determined from Equation (6) and the ion density from Equation (2). In a plasma the two are essentially the same, giving us a cross check on the measurement of  $n$ . In curve-region III, the stray electric field in the plasma due to the probe may be very large and considerable perturbation occurs.

## LIST OF REFERENCES

1. Ready, J. F., *Effects of high power laser radiation* , pp.433, Academic Press, 1971.
2. Bykovskii , yu. A ., et al., *Neutral particles from the interaction of laser radiation with a solid target* , Soviet Physics-Technical Physics, V.19, pp.1635, June 1975.
3. Chang, C. T., Hashmi, M., and Pant, H. C., *Study of a laser produced plasma by Langmuir probes* , Plasma Physics, V.19, pp.1129-1138, 1977.
4. Brooks , K . M ., *An investigation of early disturbance found in association with laser-produced plasmas* , M.S. Thesis, Naval Postgraduate School, Monterey, California, December 1973.
5. Callahan , D . J ., *Laser plasma particle velocities* , M.S. Thesis, Naval Postgraduate School, Monterey, California, June 1976.
6. Frank-Kamenetskii, D. A., *Plasma, the fourth state of material* , pp.159, Plenum Press, 1972 .
7. Chen, F. F., *Introduction to plasma physics and controlled fusion*, 2nd ed , V.1, pp.290, Plenum Press, 1984.
8. Langmuir, I., *The effect of space charge and residual gases on thermionic currents in high vacuum* , Physical Review, V. 2, pp.450-486, 1913.
9. Lochte, W., Holtgreven , *Electrical probes, in plasma diagnostics* , pp.668-731, North Holland, Amsterdam, 1968.

10. Lumonics Inc ., *Instruction manual, lumonics TE 820 HP series co<sub>2</sub> lasers* , 1976.
11. Matheson Gas Products, Inc ., *Matheson gas products catalog 88* , pp.180, 1988.
12. Laser Precision Corp ., *Rj-7000 series radiometer and Rjp-700 series probes instruction manual* , February 1984.
13. Henson, M. V., *Generation of electromagnetic radiation due to laser induced breakdown and unipolar arcing* , M.S.Thesis, Naval Postgraduate School, Monterey, California, September 1989.
14. Engel , A. V., *Ionized gases* , pp.147, Oxford, Claren-Don Press, 1965.
15. Baird, D. C., *Experimentation : An introduction of measurement theory and experiment design* , pp.198, Prentice-Hall, Inc., 1962.
16. Huddlestone , R. H., Leonard , S. L., eds. *Plasma diagnostics techniques* , pp.113, Academic Press, 1965.
17. Segall, S. B., Koopmann, D. W., *Application of cylindrical Langmuir probes to streaming plasma diagnostics* , Physics of Fluids, V.16, pp.1149, July 1973,

## INITIAL DISTRIBUTION LIST

	No. Copies
1. Defense Technical Information Center Cameron Station Alexandria, VA 22304-6145	2
2. Library, Code 0142 Naval Postgraduate School Monterey, CA 93943-5002	2
3. Prof. K. E. Woehler, Code 61Wh Department of Physics Naval Postgraduate School Monterey, CA 93943-5000	1
4. Prof. F. R. Schwirzke, Code 61Sw Department of Physics Naval Postgraduate School Monterey, CA 93943-5000	2
5. Prof. R. C. Olsen, Code 61Os Department of Physics Naval Postgraduate School Monterey, CA 93943-5000	2
6. LCDR. Youn, Duck Sang Postal Code 560-231 In Hu Dong 1 ga 171-41, Duck Jin Gu Jeon-Ju City Republic of Korea	2
7. LT. Michael V. Hensen Surface Warfare Officers School Command Newport, RI 02841-5012	1
8. Naval Academy Library Postal Code 602 Jin Hae city, Gyung Nam Republic of Korea	1

9. Naval War College Library  
Postal Code 602  
Jin Hae City, Gyung Nam  
Republic of Korea

1